Recent Trends in the Design, Synthesis, Spectroscopic Behavior, and Applications of Benzazole-Based Molecules with Solid-State Luminescence Enhancement Properties

Suzanne Fery-Forgues, Corinne Vanucci-Bacqué

▶ **To cite this version:**

Suzanne Fery-Forgues, Corinne Vanucci-Bacqué. Recent Trends in the Design, Synthesis, Spectroscopic Behavior, and Applications of Benzazole-Based Molecules with Solid-State Luminescence Enhancement Properties. Topics in current chemistry, 2021, 379 (5), pp.32. 10.1007/s41061-021-00344-8 . hal-03375318

HAL Id: hal-03375318
https://hal.science/hal-03375318v1

Submitted on 12 Oct 2021

HAL is a multi-disciplinary open access archive for the deposit and dissemination of scientific research documents, whether they are published or not. The documents may come from teaching and research institutions in France or abroad, or from public or private research centers.

L'archive ouverte pluridisciplinaire **HAL**, est destinée au dépôt et à la diffusion de documents scientifiques de niveau recherche, publiés ou non, émanant des établissements d'enseignement et de recherche français ou étrangers, des laboratoires publics ou privés.

Recent trends in the design, synthesis, spectroscopic behavior and applications of benzazole-based molecules with solid-state luminescence enhancement properties

Suzanne Fery-Forgues * and Corinne Vanucci-Bacqué

*E-mail address: sff@chimie.ups-tlse.fr

SPCMIB, CNRS UMR5068, Université de Toulouse III Paul Sabatier, 118 route de Narbonne, 31062 Toulouse cedex 9, France

Abstract

Molecules that exhibit solid-state luminescence enhancement, *i.e.* the rare property to be more strongly emissive in the solid state than in solution, find an increasing number of applications in the fields of optoelectronic and nanophotonic devices, sensors, security papers, imaging and theranostics. Benzazole (BZ) heterocycles are of particular value in this context. The simple enlargement of their π-electron system using a -C=C-Ar, or -N=C-Ar moiety is enough for intrinsic SLE properties to appear. Their association with a variety of polyaromatic motifs leads to SLE-active molecules that frequently display attractive electroluminescent properties and are sensitive to mechanical stimuli. The excited-state intramolecular proton transfer (ESIPT) process that takes place in some hydroxy derivatives reinforces the SLE effect and allows the development of new sensors based on a protection/deprotection strategy. BZ may also be incorporated into frameworks that are prototypical aggregation-induced enhancement (AIE) luminogens, such as the popular tetraphenylethene (TPE), leading to materials with excellent optical and electroluminescent performance. This review encompasses the various ways to use benzazole units in SLE systems. It underlines the significant progresses recently made in the understanding of the photophysical mechanisms involved. A brief overview of the synthesis shows that BZ units are robust building blocks, easily incorporated into a variety of structures. Generally speaking, we try to show how advantage may be taken from these small heterocycles for the design of increasingly efficient luminescent materials.

Keywords Benzoxazole . Benzothiazole . Benzimidazole . Solid-state luminescence . Aggregation-induced emission

Abbreviations

ACQ	Aggregation-caused fluorescence quenching
AIE	Aggregation-induced emission
AIE-gen	AIE-luminogen
BI	Benzimidazole
BO	Benzoxazole
BT	Benzothiazole
BZ	Benzazoles
CI	Conical intersection
DMF	Dimethylformamide
D-π-A	Electron-donor-π-bridge-electron acceptor
ESIPT	Excited-state intramolecular charge transfer
HBO	Hydroxybenzoxazole
HBT	Hydroxybenzothiazole
HOMO	Highest occupied molecular orbital
ICT	Intramolecular charge transfer
LUMO	Lowest unoccupied molecular orbitals
MFC	Mechanofluorochromism
NIR	Near infrared
OLED	Organic light-emitting diode

PL	Photoluminescence
PLQY	Photoluminescence quantum yield
PBI	Phenylbenzimidazole
PBO	Phenylbenzoxazole
PBT	Phenylbenzothiazole
RIR	Restriction of intramolecular rotations
RIM	Restriction of intramolecular motions
RACI	Restricted access to a conical intersection
SLE	Solid-state luminescence enhancement
TICT	Twisted internal charge transfer
THF	Tetrahydrofuran
TD-DFT	Time-dependent density functional theory
TPE	Tetraphylethene/tetraphenylethylene

1 Introduction

Whatever they contain one oxygen, nitrogen or sulfur bridging atom, benzazoles (BZ) are among the most relevant biologically-active heterocycles, often incorporated as building blocks in ligands to target a variety of receptors and enzymes in medicinal chemistry studies [1−4]. They are also the basic units of an important class of fluorescent organic dyes, particularly attractive due to their high quantum yield, ease of synthesis, and excellent thermal, chemical and photochemical stability. The three isologs, namely benzoxazole (BO), benzimidazole (BI) and benzothiazole (BT), have rather close spectroscopic properties governed by a stiff aromatic framework and by the presence of the heteroatoms [5]. These electron-accepting building blocks are generally connected to a π-conjugated substituent in the 2-position, and then they lead to compounds that exhibit superior luminescence properties. For this reason, all BZ units are very popular fluorescent tags of bio-conjugated molecules. They have also led to a variety of probes for the efficient detection of numerous analytes such as ions, biomolecules and explosives [6]. Distinct advantages of the BI heterocycle are its chromogenic pH sensitivity and the possibility to introduce a variety of substituents on the nitrogen atom, for example to modulate the solubility or to bring specific bio-targeting ability. As regards BO, 2-phenylbenzoxazole derivatives (PBO) have been used for a long time as near-UV dyes in scintillation counters, lasers, textile brighteners, liquid crystals and high-temperature probes [7]. Like all organic dyes, BZ derivatives have been traditionally used at small concentrations in dilute solution or after dispersion in solid matrices such as polymers. For the last two decades, they have contributed to the development of fluorescent solids made of pure organic dye molecules or containing a large amount of them. They are present in molecules that show aggregation-induced emission (AIE) properties [8, 9], and more widely speaking, solid-state luminescence enhancement (SLE) [10], *i.e.* the rare property to be more strongly emissive in the solid state than in solution. Hence they find new applications in the fields of optoelectronic and nanophotonic devices, organic solar cells, switches, sensors, security papers, biological imaging and theranostics.

The current review, which does not pretend to be exhaustive, is only focused on metal-free BZ derivatives. It begins by recalling the fundamentals of luminescence enhancement in the various solid states. Then, it explains how proper substitutions of BZ enable the emergence of intrinsic SLE properties. The association of BZ units with organic motifs chosen for their electroluminescence properties, gelation capacity, or for their response to mechanical stimuli is described. It is shown that the hydroxyl derivatives, which undergo excited-state intramolecular proton transfer (ESIPT) process, are of particular interest. This is also the case for the strongly luminescent borate complexes. Finally, the incorporation of BZ units into frameworks already well known for their AIE properties is addressed, underlining the value of these new systems. Emphasis is put on the significant progresses recently made in the understanding of the photophysical mechanisms involved. Figures gather the molecular structures together with the corresponding spectroscopic properties in a given solid state, when specified in the publications. In particular, the term “aggregates” (agg) refers to aggregates in suspension in an organic solvent/water mixture, and “powder” generally indicates a microcrystalline as-synthesized powder.

Our aim is to show the value of BZ units in the field of SLE, with the hope that this walk through multiple structures will be a source of inspiration to move towards increasingly efficient luminescent materials.

2 From emissive solids to solid-state luminescence enhancement: brief overview of a long journey

The development of organic molecules that emit light efficiently in the solid state has long been very challenging [11,12]. In fact, conventional organic fluorophores rarely exhibit this property. Even though they are excellent emitters in solution or after dispersion in a matrix, most of them become very weakly emissive at high concentrations and in the condensed state. This frequently encountered phenomenon is called aggregation-caused fluorescence quenching (ACQ). To understand its origin, it is important to consider that solid-state luminescence results from the contribution of a variety of intra- and intermolecular effects (i.e. geometrical factors affecting the molecular planarity, polarizability issues, exciton coupling and excimer formation [13, 14]) related to the molecular arrangement and to morphological features. A recent and very inspiring review from Gierschner *et al.* [15] identifies these effects and shows how difficult it is to disentangle them. Reasons for fluorescence quenching in the solid state are therefore of high complexity. Intuitively, it can be thought that the large delocalized π-conjugated moieties of organic fluorophores are prompt to stack, thus promoting non-radiative decay. Indeed, H-aggregates formed by the perfect "side by side" alignment of two molecules have been predicted to be non-emissive, but this simplified model hardly reflects the complexity of interactions between neighboring molecules in a solid. According to Gierschner *et al.*, H-aggregation is not the cause of fluorescence quenching in most of molecular solids. It is rather the trap sites, generally due to impurities and structural defects, that would play the major role in the deactivation of excited states [16].

Whatever its origin, ACQ may be circumvented by creating space between the fluorophores. To do so, fluorophores may be hosted by cyclodextrins and zeolites, or borne by macromolecules (e.g. dendrimers). According to their nature, they may be associated to bulky counterions [17−19], co-crystallized with neutral species [20−22], or chemically modified by the insertion of sterically-demanding substituents that prevent them from stacking [23]. Another strategy is to organize the aromatic moieties around a sp^3-hybridized carbon or nitrogen atom that impedes planar geometry and hence prevents π-π stacking. This strategy has proved to be very successful is the design of a new generation of dyes, the behavior of which is precisely at the opposite of that induced by ACQ. These molecules do not emit, or emit very weakly in solution, and turn to be luminescent upon aggregation and in the solid state [8,9]. This effect, first reported by Stokes in 1853, was re-discovered in 2001 by Tang *et al.*, who coined the term "aggregation-induced emission (AIE)" with the explicit goal to explore the tremendous range of applications offered by such fluorophores in the fields of fluorescent materials and probes for biology. Typical AIE-luminogens (AIE-gens) contain aromatic groups connected by rotatable C-C, C-N or N-N single bonds. They are often propeller or spiro-shaped compounds. It was first accepted that fluorescence quenching in solution results from the waste of excitation energy *via* thermal processes linked to rotations and large molecular motions. The restriction of intramolecular rotations (RIR) and motions (RIM) that occurs in the solid state was then assumed to be responsible for AIE. Indeed, the photophysical mechanisms involved are much more complex, although molecular stiffening is still at the basis of fluorescence revival [10]. Advances from theoretical chemistry have recently given another perspective on the AIE phenomenon. They have shown that the geometry of typical AIE-gens in a fluid medium may vary considerably under excitation, taking the molecule very far from the ground-state equilibrium structure. The potential energy surfaces of the ground and excited states that correspond to this geometry are close to each other. They are degenerate and almost intersect in a region called conical intersection (CI). The probability to pass from the excited state to the ground state *via* non-radiative internal conversion is therefore maximal in this region. In contrast, in rigid medium where the molecular motions are impeded, the CI is no longer thermally accessible, and deactivation *via* the emission of light is strongly enhanced (Fig. 1). This restricted access to a conical intersection (RACI) model, introduced by Blancafort, Crespo-Otero *et al.*, is now widely accepted to account for the behavior of AIE-gens

[24−26]. Furthermore, the group of Ciofini and Adamo has shown theoretically that considering the electrostatic field induced by the environment at the excited state can be enough to explain the brightness enhancement and shift of the emission wavelength observed for an AIE-gen in the crystalline state, in comparison with dilute solutions [27].

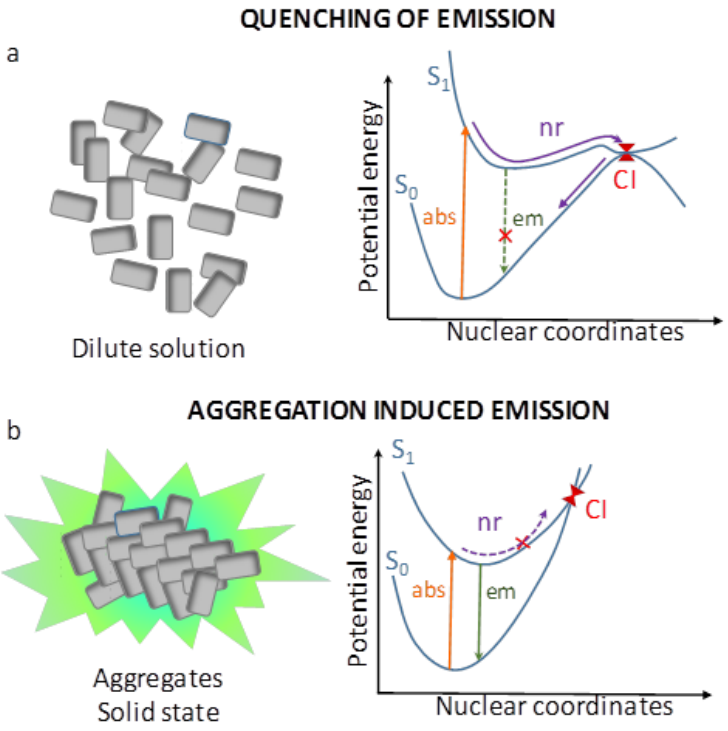

Figure 1. Left: Representation of typical AIE-active fluorophore molecules in dilute fluid solution (a) and in the aggregate and solid states (b). Right: For each case, schematic description of the absorption (abs), emission (em) and non-radiative (nr) processes along the potential energy surface curves of the ground state (S_0) and first excited singlet state (S_1). Conical intersections (CI) are indicated in red ink.

The stiffening of the structure is not the only prerequisite for emission to be observed in the solid state. Fluorophores must adopt a molecular geometry that promotes the emission of light, and arrange between them in a favorable way. The initial AIE label paid little attention to these interactions because it mainly referred to phenomena observed with the formation of aggregates. Consequently, the term "solid state luminescence enhancement" (SLE) now seems to be more appropriate to consider the whole set of intra- and intermolecular factors involved in solid-state emission, and to encompass the various solid states, which range from highly viscous or solid solutions to amorphous powders and crystals [10].

Generally speaking, it must be kept in mind that any change in the molecular conformation and in the supramolecular organization may induce variations in the photoluminescence (PL) color and/or intensity [28, 29]. It is possible to play on these factors by non-covalent approaches, the merit of which is to reduce the effort in synthesis and to make the best from a given fluorophore [11, 30]. For instance, polymorphism, i.e. the ability of a molecule to adopt different crystal structures, provides many opportunities to tune the optical properties just by implementing various conditions of crystallization [31−33]. Some fluorescent organic molecules also show variations in their PL properties in response of a physical stimulus, in particular mechanical stress, in other words they exhibit mechanofluorochromism (MFC) [14, 28, 34−38]. Typically, emission is changed by grinding, rubbing, crushing, pressing, shearing, or smearing, and the molecules are restored to their original state by annealing or fuming by solvent vapors, which increase the molecular mobility. The molecular chemical structure is not affected. This phenomenon is attributed to subtle and reversible changes in molecular conformation and planarity, or in the crystal packing mode. It often results from phase

transition between crystalline phase to amorphous phase, under mechanical forces. A prerequisite is that the molecular stacking in the crystal state is loose and can be easily destroyed under mechanical stress, resulting in a transformation of the emission properties. This is the reason why MFC is frequently associated to SLE materials. From a general viewpoint, the development of such mechanofluorochromic compounds is an emerging field of research that leads to smart materials for the detection of stress in polymers, security inks, data storage and memory devices. Finally, it must be underlined that the modifications undergone by one molecule or one group of molecules may impact a large number of surrounding molecules. The response to a stimulus is then amplified in the solid state with respect to dispersed molecules [39, 40], a collective behavior that may be of great value for sensing materials.

Benzazole derivatives have taken part in the epic development of photoluminescent materials. However, some molecular engineering is necessary to bestow the BZ units with SLE behavior.

3 The emergence of AIE behavior in small benzazole derivatives

3.1 From dicyanovinyl derivatives to styryl dyes

Aryl-benzazoles belong to a family of dyes that spontaneously adopt solid-state arrangements compatible with efficient fluorescence emission. Even for the smallest molecules, the PL properties are often good. For example, the photoluminescence quantum yield (PLQY) of 2-phenylbenzoxazole (PBO) is 0.26 and that of the 4-methoxy derivative is 0.38, with emission maximum at 360 nm and 382 nm, respectively [7, 41]. These molecules are also very strongly emissive in solution, and so they do not show any SLE behavior. The adequate extension of the π–conjugated system not only shifts the emission to the visible range, but frequently endows the molecule with SLE properties. This effect may be enhanced by the presence of at least one cyano group, a classical electron acceptor that has been identified for a long time as a key factor in the creation of supramolecular interactions, leading to strongly fluorescent SLE-active organic materials (Fig. 2) [42].

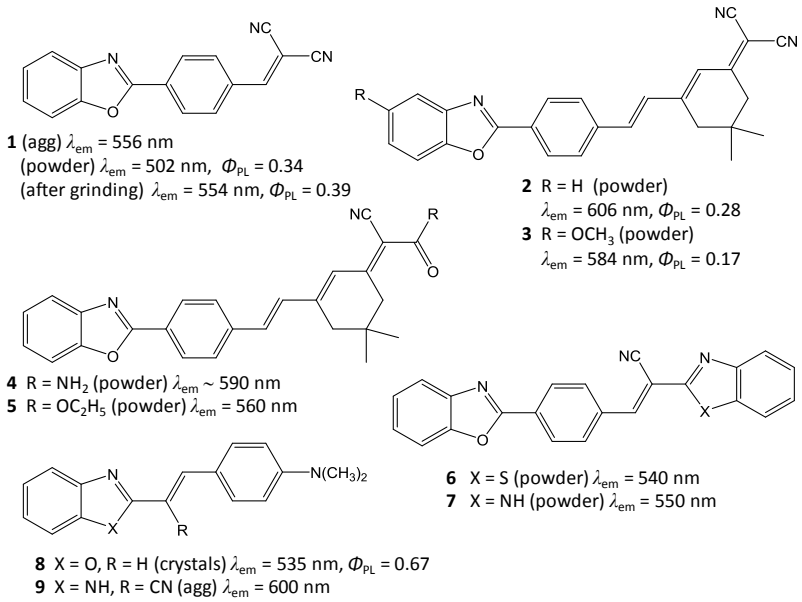

Figure 2. Molecular structure of compounds **1** [43], **2** and **3** [45], **4**–**7** [44], **8** [49] and **9** [50,52] with solid-state PL maxima (λ_{em}) and photoluminescence quantum yields (Φ_{PL}).

The dicyanovinyl-PBO derivative **1** developed by our team is probably the smallest benzazole-based molecule endowed with SLE properties [43]. This molecule is weakly emissive in the blue region in pure THF solution. By increasing the proportion of water in a THF/water solution, the emission is first shifted from blue to turquoise. Then, above 80% water in the medium, opacification

of the medium occurs with emission of strong yellow light with maximum at 556 nm (Figure 3a). Observation with the fluorescence microscope of the suspension with 95% water shows that emission arises from small fluorescent microcrystals (Fig. 3b). The PLQY of the microcrystalline powder is 0.34, from 11 to 16 folds higher than in organic solutions. It is noteworthy that the relatively small chemical modification brought to PBO has allowed the PL spectrum to be shifted from the near UV to the first half of the visible range.

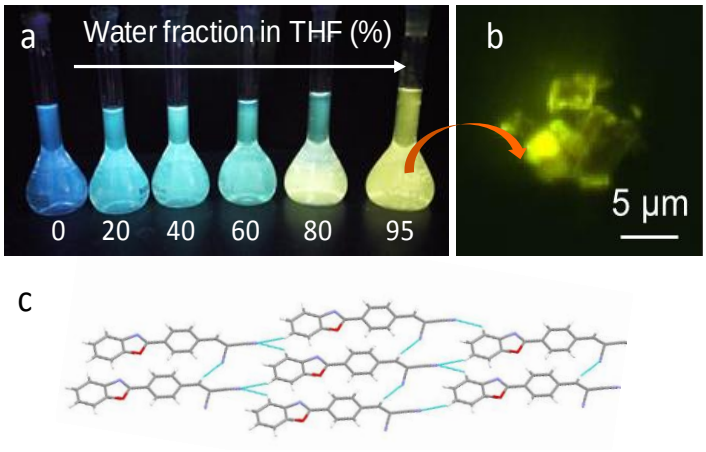

Figure 3. a) Samples of compound **1** (2.6×10^{-5} M) in pure THF and various water/THF mixtures containing 20, 40, 60, 80 and 95% water upon illumination by a UV lamp at 365 nm. b) Fluorescence microscopy image of **1** in water/THF 95:5 mixture (λ_{ex} = 450-490 nm, λ_{em} > 500 nm). c) Crystal packing of molecules of **1** forming a layer. Short contacts are highlighted in turquoise.

In microcrystals, strong N···H-C hydrogen bonds are formed between the cyano groups and the hydrogen atoms of the vinylene unit and BO ring of adjacent molecules. As a result, molecules form layers (Fig. 3c), prone to slip with respect to each other upon mechanical stimuli. A mechanofluorochromic behavior was indeed observed. The pristine microcrystals emit yellow-green light (502 nm), which becomes golden yellow (554 nm) upon grinding, and *vice versa* by heating or solvent fuming. This phenomenon was accompanied by a reversible evolution of the photoluminescence quantum yields and lifetimes. These variations were attributed to the formation of different types of emissive species in the crystalline phases and in the ground material, which is a mixture of very small microcrystals and amorphous matter. Remarkably, evidence was given for additional spectroscopic effects, which may be easily confused with MFC, but actually depend on the size, compactness and heterogeneity of the solid samples. These effects are presumably linked to the generation of regions rich in low-energy exciton traps in polycrystalline and pressed samples, and to reabsorption of light.

In compound **2** introduced by Yadav *et al.* [44] and subsequently studied by our group, the dicyanomethylene group is integrated into a rigid and bulky dimethylcyclohexene moiety. The enlargement of the π-electron system results in a significant red shift of the excitation and emission spectra with respect to **1**, and in the enhancement of the SLE effect. This compound is indeed very weakly fluorescent in fluid organic solvents, but fluorescence intensity increases with increasing viscosity, and the PLQY reaches 0.28 in the solid state (Fig. 4a)[45]. When increasing the proportion of water into a THF solution of **2**, the emission intensity at the PL maximum wavelength (584 nm) is strongly enhanced up to 45 folds (Fig. 4b,c). Scanning electron microscopy show the presence of micrometer-sized amorphous particles, some of them resembling empty rice grains, at fw = 60%, while the sample at fw = 95% contained agglomerates of cubic microcrystals measuring several hundreds of nanometers (Fig. 4d,e). The presence of a methoxy group on the BO ring (compound **3**) does not enhance the SLE behavior, while the substitution by a hydroxy group is strongly detrimental to PL emission in the solid state. No clear MFC effect was detected for molecules **2** and **3**, which arrange in densely packed crystal networks [45].

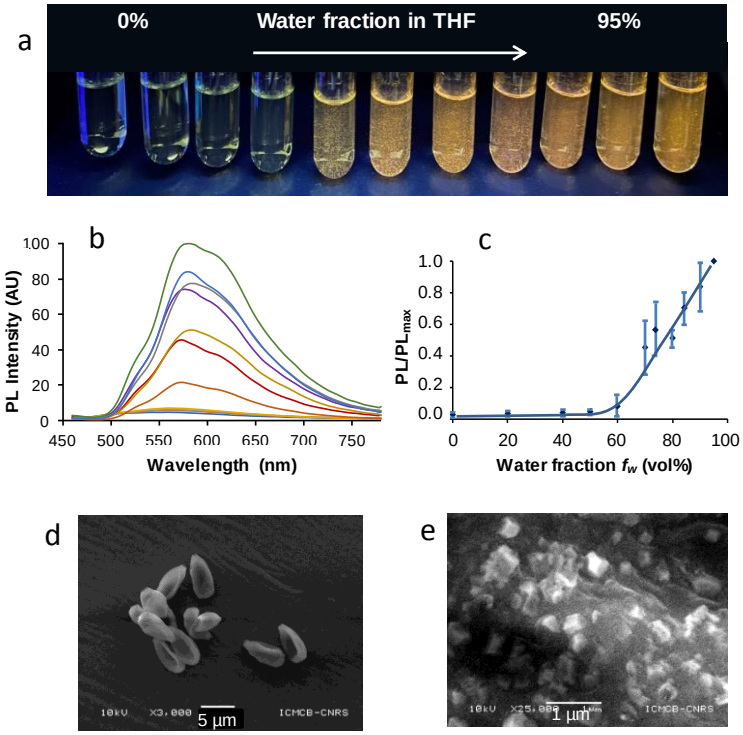

Figure 4 a) Samples of dye **2** (~7 × 10^{-6} M) in various THF/water mixtures, illuminated by a hand-held UV lamps (365 nm). b) Corresponding PL spectra with λ_{ex} = 440 nm. c) Plot of the PL intensity ratio at 586 nm versus the water content in the solvent mixture (average of 3 measurements). Scanning electron microscopy images of the suspensions at f_w = 60% (d) and 95% (e).

Yadav *et al.* [44] have also reported compounds **4** and **5** with only one terminal electron-withdrawing cyano group. The stilbenic derivatives (**6** and **7**) combine PBO with BI and BT, with the cyano group placed at the center of the molecule. Theoretical calculations show that, for all these molecules, the highest occupied molecular orbitals (HOMO) are mainly located on the benzazole moieties, and the lowest unoccupied molecular orbitals (LUMO) are centered on the cyano groups. All these molecules display SLE properties with intense emission in the solid state, varying from yellow to orange according to the position and strength of the electron withdrawing group. These compounds are extremely stable, from a thermal and photochemical point of view.

As for the mechanism, the PBO group is quite rigid at room temperature, and rotations between the phenyl and BO moieties do not play a major role in the spectroscopic behavior. However, it may be considered that molecules **1**, **2** and **3** are molecular rotors in fluid solution, like many compounds bearing a terminal dicyanovinyl group. The dicyanovinyl moiety of **1**, and the 5,5-(dimethylcyclohex-2-en-1-ylidene)malononitrile moiety of **2** may rotate around the single bond, thus generating large molecular motions. This type of rotation leads to a dark twisted internal charge transfer state (TICT) [46]. It has been shown for a long time that a closely-related molecule undergoes an irreversible twist around the dicyanomethylene bond, which allows reaching a thermally accessible CI [47]. For all molecules **1**−**7**, the structural similarity to stilbenoid systems suggests that a twist around the vinyl double bond, due to the photochemical formation of a bi-radical species precluding the possibility of *cis-trans* isomerisation, would allow reaching the CI [48]. The rigidification due to the formation of aggregates and microcrystals would prevent these two non-radiative deactivation pathways, thus explaining the enhanced PL emission.

Regarding stilbenic derivatives, reference compound **8** has clear electron-donor-π-bridge-electron acceptor (D-π-A) character due to the presence of a strong electron-donating *N*,*N*-dimethylamino group. This compound is very weakly emissive in organic solvents, whereas crystals strongly emit in the yellow green (535 nm) with PLQY as high as 0.67. Crystal film responds reversibly to volatile acid vapours, protonation occurring successively on the two nitrogen atoms of this PBO derivative [49]. In compound **9** studied by Horak *et al.*, the cyano group close to the BI

moiety reinforces the electron withdrawing effect on this side of the molecule [50]. In water, this compound forms aggregates that emit orange-red fluorescence, the intensity of which is approximately 35-fold the emission of dissolved molecules in ethanol. The strong push-pull character of the molecule is probably responsible for the emission at long wavelength (600 nm). On alternate exposure of **9** in solid state to the vapours of HCl and NH_3, the emission is switched on and off [51]. The luminescence of the aggregates formed in aqueous organic solvent is quenched in the presence of picric acid, and so the compound has been proposed for the sensitive detection of nitroaromatic explosives [52]. Interestingly, the derivative in which the BI nitrogen atom is substituted by a phenyl ring does not show any SLE property. It seems that for stilbenic derivatives, the cyano group acts more as an auxochrome rather than as a SLE promoter. RIR and planarization have been evoked to explain the SLE effect. Besides, as shown with a BT analogue of **8**, the main deactivation mechanism of these compounds in fluid solvents is a photoisomerization, the restriction of which leads to the increase in fluorescence quantum yield in viscous solvents [53]. It is likely that the same process takes place in the solid state.

3.2 Schiff base derivatives

The Schiff bases **10**−**12** (Fig. 5) studied by the group of Zhou are isomers, differing by the position of the nitrogen atom in the distal pyridine group. They have a twisted conformation due to steric hindrance between the rings and do not present significant push-pull character. The emission maximum of powders is centered between 471 and 495 nm, according to the compound. These dyes are much more emissive as aggregates and amorphous powders than in the crystalline state. This behavior is attributed to a detrimental crystal packing mode in which the molecules stack together face-to-face, with extensive overlap of their aromatic systems [54]. In contrast, the presence of a *N,N*-diethylamino group in **13** prevents π-π stacking and induces cross packing arrangement, resulting in particularly emissive crystals. This electron-donating group also contributes to the push-pull effect, so that the emission maximum is around 593 nm in crystals, and 552 nm in a powder of low crystallinity [55].

In comparison with **13**, the Schiff bases **14**−**16** of Horak *et al.* have a small π–conjugated system [56]. The intramolecular charge transfer (ICT) is reinforced by replacing the methyl group at the BI acceptor moiety by the strong electron withdrawing CN and NO_2 groups. The solid state emission is then tuned from 525 nm to 571 and 580 nm, respectively.

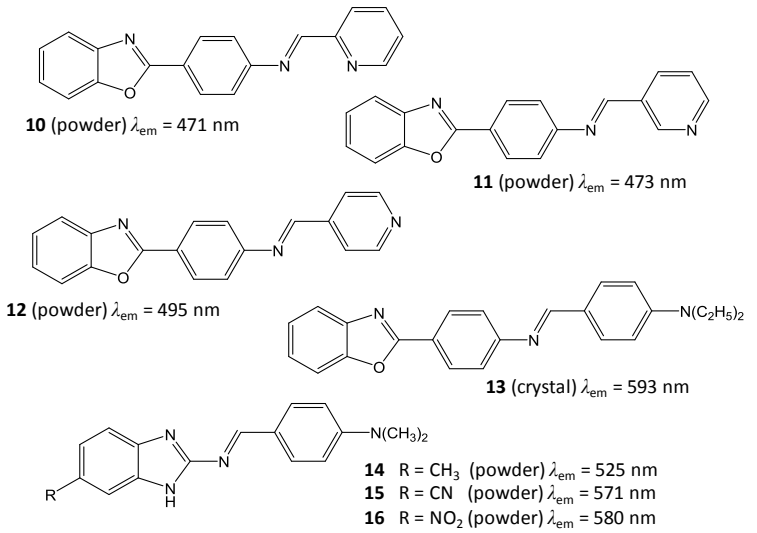

Figure 5. Molecular structure of Schiff base derivatives **10**–**12** [54], **13** [55] and **14**–**16** [56] with solid-state PL maxima (λ_{em}).

In molecules **17** and **18**, the PBI moieties are connected to the Schiff base by an aliphatic linker (Fig. 6) [57, 58]. Like many molecules that contain amide, amino acid, or urea moieties, these compounds form organogels with low minimum gelation concentration. They show strong SLE effect. For instance, in a mixed solvent of dimethylsulfoxyde and ethylene glycol, **17** produces a dense, blue-emitting 3D-network of entangled fibres stabilized by hydrogen bonds. The incorporation of Cd^{2+} cations leads to a metallogel that involves coordination interactions and emits brilliant blue light. The gel can turn back to a weakly emissive liquid-like material after heating, and *vice versa* [57].

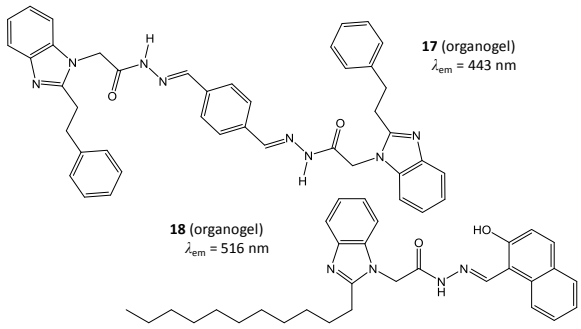

Figure 6. Molecular structure of organogelators **17** [57] and **18** [58] with solid-state PL maxima (λ_{em}).

The formation of the organogel from compound **18** in a glycerol/ethylene glycol mixture is accompanied by the emission of strong brilliant yellow-green fluorescence. This gel is stabilized by numerous interactions, i.e. hydrogen bonds between the acylhydrazone and the hydroxyl groups, π-π stacking interactions between the naphthyl moieties, and strong van der Waals interactions taking place between the long alkyl chains. Addition of CN^- anions and Al^{3+} cations lead to a fluorescent and colorimetric response, with good selectivity with respect to other ions. The presence of Fe^{3+} quenches fluorescence that may be recovered by addition of L-cysteine. This "smart" gel can then act as a "on-off-on" fluorescence switch, potentially usable as an erasable fluorescent display (Fig. 7) [58].

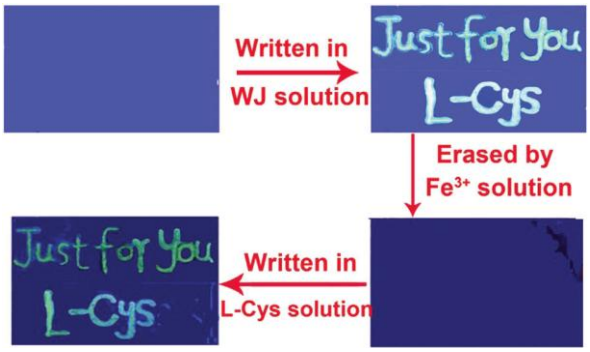

Figure 7. Photographs of **18** on test film taken under exposure with a UV light (365 nm). A solution of **18** (2.0×10^{-2} M) was used to write on a silica gel plate, and let to dry in the open air. The test plate was then brushed with a solution of Fe^{3+}, then dipped into a water solution of L-Cys. Reproduced from Ref. 58 with permission from the Royal Society of Chemistry.

3.3 Carboxamide derivatives

There is no π-conjugation between the PBO unit and the rest of the molecule in the carboxamide derivatives **19** and **20**, which are two positional isomers (Fig. 8). The molecular backbone is very flexible. Both compounds mainly emit in the blue in the condensed state, with small color changes depending on the degree of crystallinity. Isomer **19**, in which the 4-*tert*-butylbenzamide group is

connected to the 3'position of the PBO moiety, is almost not emissive in fluid organic solvent and only weakly emissive as a powder (Φ_{PL} = 0.09). SLE is attributed to RIR that locks the molecule in an emissive quasi-TICT exited state, formed through incomplete transition of the local excited state to a dark TICT state. The RIR effect is supposed to increase with the order of the molecular arrangement, i.e. amorphous film < nanosheet < powder < crystalline state, and this could explain that the PL efficiency varies similarly [59]. In contrast, isomer **20**, in which the 4-*tert*-butylbenzamide group is placed in the 4'position of the PBO moiety, is strongly emissive. The PLQY of the powder is close to 0.50, almost 230 times higher than in THF solution. In this case, the mechanism was attributed to restriction of non-radiative TICT. A major contribution of the crystal packing mode, in which molecules adopt the cross dipole stacking typical of PBO [7], is also evoked to explain the spectacular SLE effect [60].

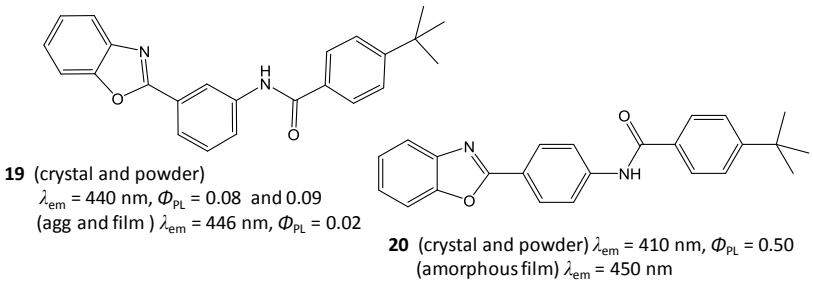

Figure 8. Molecular structure of carboxamide derivatives **19** [59] and **20** [60] with solid-state PL maxima (λ_{em}) and photoluminescence quantum yields (Φ_{PL}).

3.4 2'-Hydroxy-derivatives: exploiting the ESIPT effect for ultra-sensitive sensing

When a proton-donating hydroxyl group is in close proximity to a heteroatom that acts as a proton acceptor, an intramolecular hydrogen bond may take place. Such molecules exhibit conformational tautomerism, and lead to a special photophysical process, i.e. excited-state intramolecular proton transfer (ESIPT) [61]. ESIPT is characterized by the presence, in addition to fluorescence at short wavelengths due to the enol form, of an intense fluorescence emission at long wavelengths due to the keto form, with an anomalously large Stokes shift. It is an extremely fast process, able to appear even in rigid glass at very low temperature and in the solid state, and it leads to remarkable solid-state emitters [62]. As recently reviewed by Sedgwick *et al.*, ESIPT and SLE processes are closely related [63]. The RIM and molecular planarization that result from transition to the solid state facilitate the formation of the intramolecular hydrogen bond and generally promotes the ESIPT process. Conversely, the strong emission of the excited keto form enhances the solid-state emission with respect to solutions (Fig. 9).

The 2-(2'-hydroxyphenyl)benzazole framework is a conventional ESIPT pattern. Its smallest derivatives are AIE-fluorogens. For instance, 2-(2'-hydroxyphenyl)benzoxazole (HBO) **21** emits at 504 nm in its crystalline form, with a PLQY of 0.42, a value multiplied by 23 with respect to solutions [64] (Fig. 10). Its derivative bearing a small amido substituent **22** also emits near 500 nm [65]. The hydroxybenzothiazole (HBT) analogue **23** emits at 509 nm, aggregates have a PLQY of 0.27, nearly 15-fold higher than in cyclohexane. Ultrafast transient absorption spectroscopy showed that for **23** the observed SLE effect results from the combination of intermolecular interactions and RIM, which play opposite roles on PL emission [66].

The HBO fragment has allowed the construction of ratiometric fluorescent probes, using a phenolic hydroxyl protection/deprotection strategy. Compound **24**, which differs from **22** by the presence of a long alkyl chain, emits weak violet emission in dimethylsulfoxide solutions arising from the enol form, while the strong emission around 500 nm in the solid state comes from the keto form.

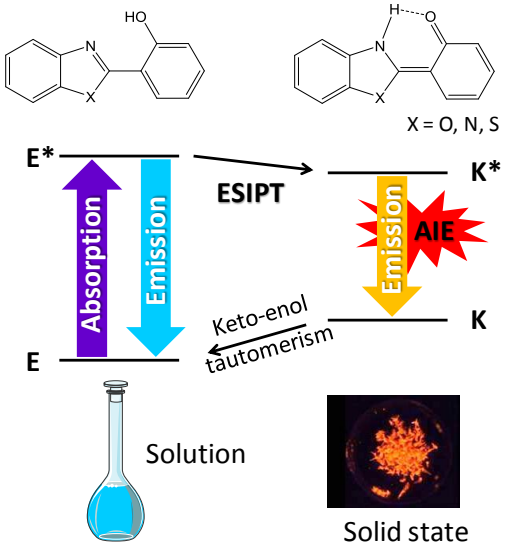

Figure 9. Simplified schematic representation of excited-state intramolecular proton transfer (ESIPT) process combined with SLE for a phenyl-benzazole derivative. E: enol form, K: keto form.

Caged compound **25**, where the hydroxyl group is protected with a boronate-benzyl group, only emits in the violet (405 nm) when dispersed in cationic surfactant cetyltrimethylammonium bromide (CTAB) below the critical micelle concentration (CMC). Reaction with hydrogen peroxide H_2O_2 regenerates compound **24** and yellow emission with a PLQY of 0.37 attributed to ESIPT appears. The following system has been proposed as a ratiometric sensor of H_2O_2 [65].

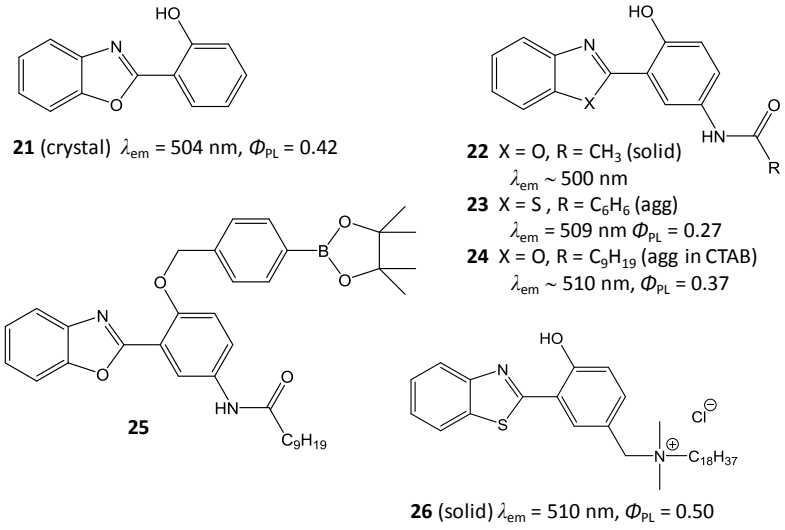

Figure 10. Molecular structure of compounds **21** [64], **22** [65], **23** [66], **24** and **25** [65], **26** [67] with solid-state PL maxima (λ_{em}) and photoluminescence quantum yields (Φ_{PL}).

Another interesting application has been reported for the cationic molecule **26**, which interacts with anionic surfactants in water to form highly emissive catanionic aggregates with increased keto/enol emission ratio. Owing to the affinity of the probe for negatively-charged bacterial cell walls, the light-up fluorescence was also used for imaging *E. coli* bacteria according to a wash-free procedure [67,68].

Due to the simultaneous presence of the HBO unit, urea group and two long alkyl chains, molecule **27** establishes a variety of weak intermolecular interactions. In a toluene-rich organic

medium, this molecule forms a colorless gel, strongly emissive in the green under UV light, with fluorescence intensity 26 times greater than in solution. Upon addition of fluoride anions, the gel turns green, probably because of direct interaction between fluoride anions and the hydroxyl group of HBO, and it is disrupted, which is attributed to concomitant deprotonation of the urea groups. The system is then a naked-eye fluoride sensor that shows both gel-to-sol transition and a visibly noticeable color change, with good selectivity with respect to other anions [69].

The dendritic compound **28** is also able to participate to multiple weak interactions. In a variety of organic solvents, it forms gels constituted of fibers and ribbons of different sizes. The SLE effect upon gelation is clear. The presence of fluoride anion causes the gel disruption, due to interactions with the hydroxyl group that play a crucial role in the gelation process. Other external stimuli (i.e. addition of zinc cations, pH changes, shear stress and sonication) have been used to trigger the phase transition of the gel, on a reversible way. It is proposed that these variations could be monitored by fluorescence spectroscopy and that the system could evolve towards a multiresponsive fluorescent sensor [70].

Although it does not contain any fatty chain or dendritic structure, compound **29** also forms very stable gels in THF/cyclohexane mixed solvents, in which molecules are arranged as nanobelts [71]. In all these gelator systems, the SLE phenomenon is attributed to the combination of *J*-aggregation, fast ESIPT process and restriction of TICT.

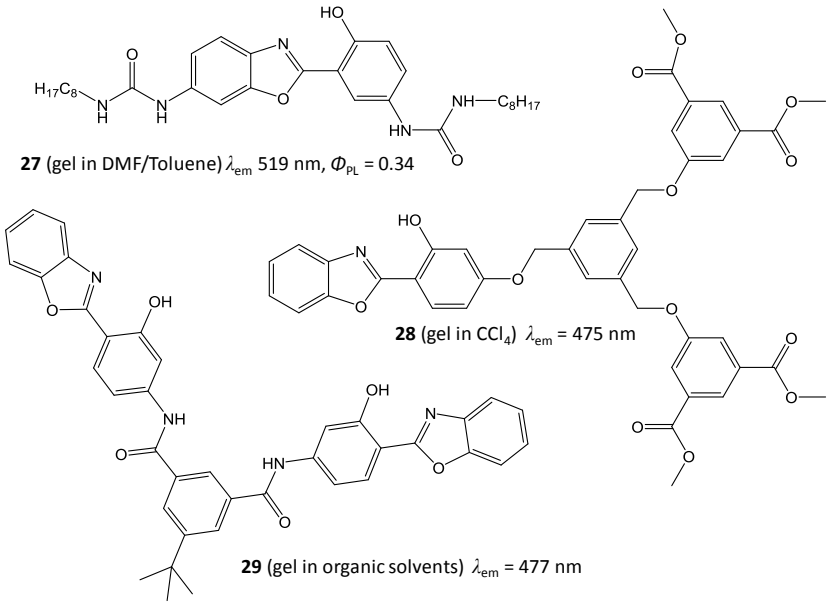

Figure 11. Molecular structure of ESIPT-active organogelators **27** [69], **28** [70] and **29** [71] with solid-state PL maxima (λ_{em}) and photoluminescence quantum yields (Φ_{PL}).

The rigidified π-extended HBO derivatives **30**–**36** (Fig. 12) have been prepared in the team of Ulrich and Ziessel. The proton donor is borne by a benzofuran fragment. The PLQY of the compounds is between 0.08 and 0.54, systematically higher than in solutions. The E*/K* ratio was fine-tuned by the substitution pattern of the molecule, with maximum emission between 476 to 580 nm. Dual emission was observed in amorphous powders, resulting in the production of white light, of great interest for electroluminescent devices [72].

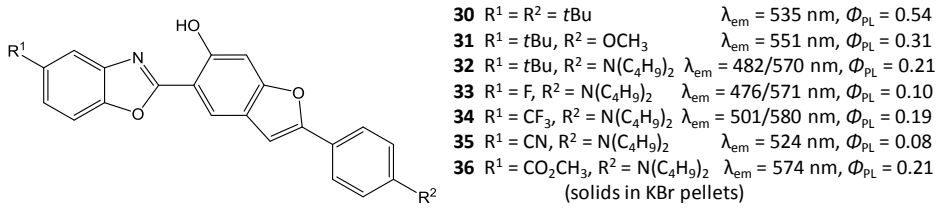

Figure 12. Molecular structure of ESIPT-active compounds **30**–**36** [72] with solid-state PL maxima (λ_{em}) and photoluminescence quantum yields (Φ_{PL}).

In the following molecules, the proton acceptor group is the nitrogen atom of the Schiff base. The PBO derivatives **37** and **38** (Fig. 13) emit faint blue light in solutions, and strong yellow light in crystals. Compound **37** gives fibers and needle-like crystals, with cross-packing layer structures. Of course, the parent compound **13**, deprived of hydroxyl group, does not exhibit this behavior. In the solid-state, the yellow emission of **37** turned blue upon exposure to vapors of dichloromethane, chloroform and tetrahydrofuran, and *vice versa* after removing the vapor. The molecule could then be used as a sensor to detect volatile organic solvents [55]. The BT derivative **39** is virtually not emissive in common organic solvents and it emits yellow light at 540 nm in the solid state [73].

With their extended π-conjugated system and D-π-A structure, the BI derivatives **40** and **41** have been designed so that emission is shifted to the red region. However, the ESIPT process does not reinforce systematically the expected effect. By comparison with their respective parent compounds **15** and **16**, the ESIPT-active cyano-substituted derivative **40** emits at shorter wavelengths (536 *vs* 571 nm), while the nitro-substituted derivative **41** emits at much longer wavelengths (620 *vs* 580 nm). The later compound also shows neat MFC behavior [56].

It will be seen below that advantage may be taken from the ESIPT process in other types of molecules.

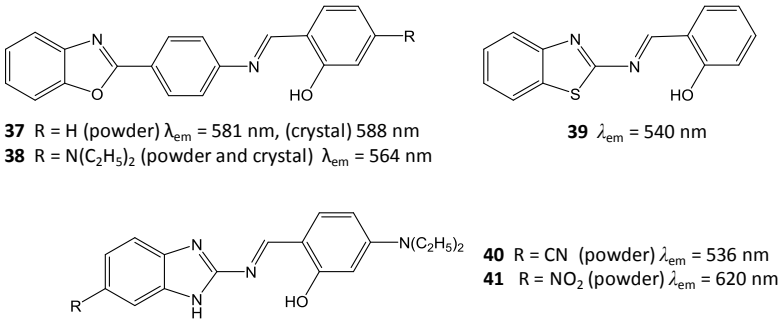

Figure 13. Molecular structure of ESIPT-active Schiff bases derivatives **37** and **38** [55], **39** [73], **40** and **41** [56] with solid-state PL maxima (λ_{em}) and photoluminescence quantum yields (Φ_{PL}).

3.5 Fluorene derivatives: En route for applications as electroluminescent materials

The combination of BZ moieties with polyaromatic compounds that have special physicochemical properties is expected to give new functional materials. For example, fluorene and its derivatives have desirable electron transporting properties and they are among the most studied electroluminescent materials for applications in optoelectronic devices. In molecules **42**–**46** (Fig. 14) developed by Padalkar *et al.*,the BZ unit act as an electron-withdrawing group, controls the crystal packing mode and brings efficient ESIPT properties. The study of the AIE behavior performed on compound **43** shows that aggregates emit 7-fold more than solutions. For all these molecules, thin films obtained by spin-casting from dichloromethane solution have excellent PLQY, up to 0.67. The size of the alkyl chain of the BT derivatives **42**–**45** has relatively small effect of the optical properties [74]. These fluorene derivatives are good candidates for electroluminescence applications.

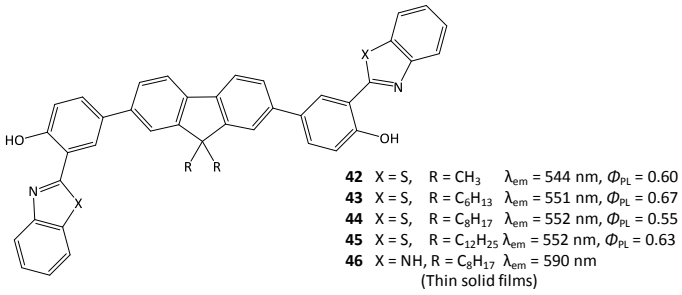

Figure 14. Molecular structure of fluorene derivatives **42**–**46** [74] with solid-state PL maxima (λ_{em}) and photoluminescence quantum yields (Φ_{PL}).

3.6 Carbazole derivatives: electroluminescence and gels

This is also the case for the carbazole derivatives **47**–**49**. Carbazoles are known for their hole-transporting properties. They are strong electron donors, with good thermal stability. Like most of organic dyes, their fluorescence is quenched upon aggregation. However, the association with HBT units allows obtaining D-π-A compounds that display excellent SLE properties, boosted by the ESIPT effect. For instance, molecules **47**–**49** (Fig. 15) are three positional isomers based on carbazole and HBT. They are strongly emissive in the green region. The PLQY reaches 0.38 for **47**, but is lower for the other two compounds, due to conformational differences [75].

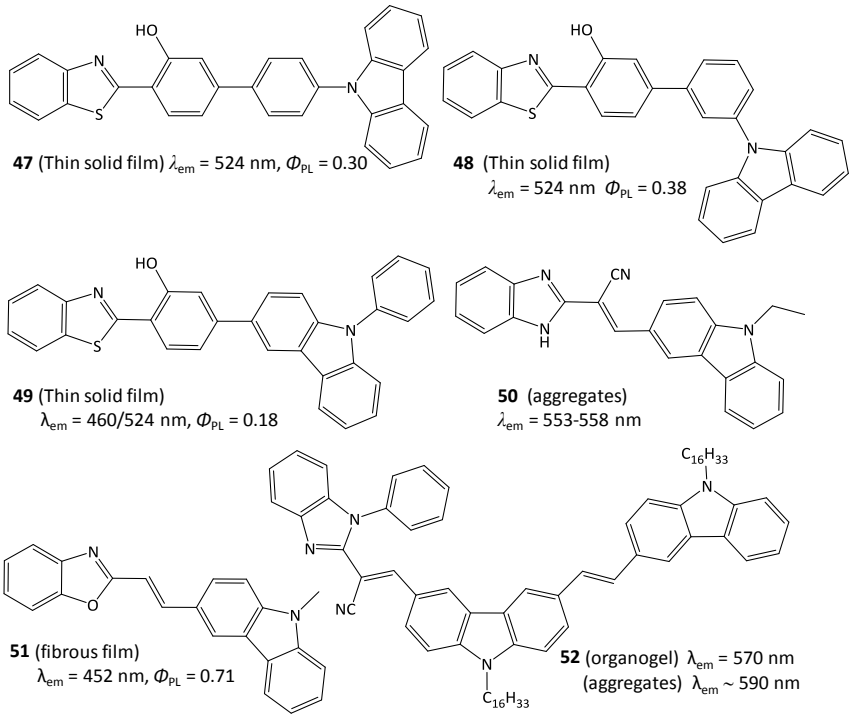

Figure 15. Molecular structure of carbazole derivatives **47**–**49** [75], **50** [52], **51** [77] and **52** [78] with solid-state PL maxima (λ_{em}) and photoluminescence quantum yields (Φ_{PL}).

Of course, carbazoles may also be used only as an electron-donating substituent. By this regard, molecule **50** behaves similarly to the *N*,*N*-dimethylaminophenyl analogue **9**, and is also suitable for the detection of picric acid [52].

However, the benzoxazole and carbazole conjugates present additional properties. Compound **51** investigated by Xue *et al*. self-assemble into strongly emissive long fibers. Upon application of mechanical shearing to the fibrous film, the photoluminescence passed from bright blue to blue-green and the intensity of emission decreased. The initial signal was progressively restored at room temperature. In contrast, the exposure to volatile acetic acid induced the emission of orange light and a heat treatment was required to regenerate the film. The acidic vapors selectively act as a stabilizer and developer to retain the information imparted by mechanical forces [76]. Molecule **51** was also reported to be a gelator in organic solvents. The emission intensity of gel increased 16-fold with respect to solutions, with a PLQY reaching 0.71 [77]. In a similar way, molecule **52** reported by Wu *et al.* gelates *n*-butanol with critical gel concentration as low as 1.8×10^{-3} M, making it a super gelator. Beside the acid-sensitive PBI unit, this molecule contains two carbazole units, one of them bearing a long alkyl chain to favor gelation, and a cyanovinyl linker for enhancing the AIE properties. Indeed, aggregates and gels emit strongly in the yellow region while fluid solutions almost not emissive. After drying, the gels give nanofibre-based thin films, the PL of which is quenched by exposure to trifluoroacetic acid. These xerogels could be used as turn-off type fluorescent sensory material for the detection of volatile acids [78].

3.7 Phenothiazine derivatives

MFC can also be enhanced by conjugating BZ units with nonplanar π-conjugated molecules such as phenothiazine, which has a bowl-shape configuration and leads to lose molecular stacking. Molecules **53** and **54** (Fig. 16) are very emissive in the solid state, but probably weakly or not SLE-active because their fluorescence quantum yield in solution is quite high. However, they are an interesting example of MFC-active molecules. Grinding of films induced a PL red shift, particularly significant for the bromine derivative. More interestingly, the ground film of **53** could rapidly self-heal at ambient temperature, while heating or solvent fuming was necessary for the ground film of **54** to revert into the original one [79].

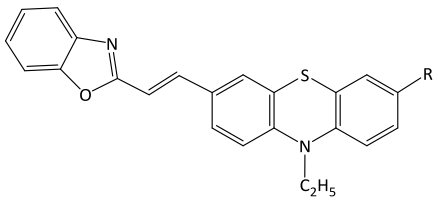

53 R = H (pristine crystals) λ_{em} = 537 nm
(after grinding) λ_{em} = 567 nm
54 R = Br (pristine crystals) λ_{em} = 529 nm
(after grinding) λ_{em} = 557 nm

Figure 16. Molecular structure of phenothiazine derivatives **53** and **54** [79] with solid-state PL maxima (λ_{em}).

3.8 Triphenylamine derivatives

Owing to its good hole-transporting capabilities, triphenylamine (TPA) has frequently been incorporated into dyes designed for use in electroluminescent devices such as dye-sensitized solar cells and organic light-emitting diodes (OLEDs). It is a popular electron donor. Its fluorescent derivatives are generally well emissive in solution, but suffer from the ACQ effect, despite the fact that TPA has a propeller shape that can prevent intermolecular π-stacking. For the last decade, significant efforts have been made to transform TPA derivatives into AIE-gens [8]. The association with BZ is a simple and convenient way to reach this aim.

Compound **55** (Fig. 17) is moderately emissive in organic solution, and its pristine crystals emit strongly in the blue-green region. Upon grinding, the compound exhibited low-contrast PL color change, with a modest spectral shift of 29 nm towards long wavelengths. Interestingly, the protonated compound exhibited high contrast piezofluorochromism with a large spectral change of 75 nm, and this finding shows the advantage of combining an external chemical stimulus with MFC [80].

The A-π-D-π-A compounds **56** and **57** of Padalkar *et al.* contain two PBT units connected to TPA. Although they differ by the absence or presence of one ESIPT unit, both compounds have

similar spectroscopic properties. To explain this unexpected finding, the authors hypothesize that the ESIPT process is dominated by the ICT process. [81].

In the parent D-π-A structures **58**–**60**, the presence of the ESIPT motif in **59** leads to dual emission in the solid state, not observed for the other compounds. However, the PLQY of **59** is much lower than for the non-ESIPT analogues, probably because of detrimental conformation [82]. All these compounds are more strongly emissive in organic solvents than in the solid state, but it may be considered that an SLE effect is detected with respect to water-containing solvents that quench fluorescence. Remarkably, the PLQY of dye **60** is up to 0.88 (solid film).

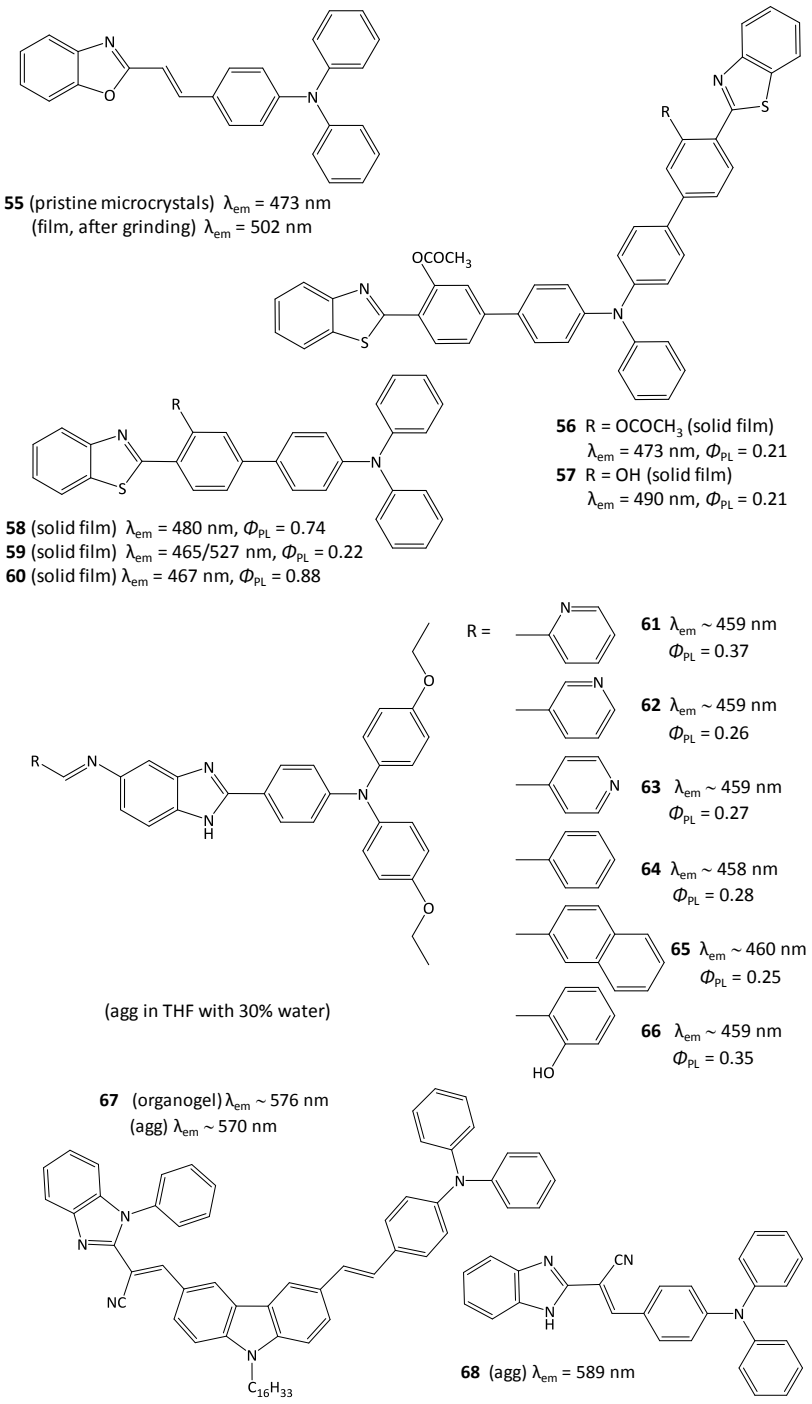

Figure 17. Molecular structure of the triphenylamine derivatives **55** [80], **56** and **57** [81], **58**–**60** [82], **61**–**66** [83], **67** [78] and **68** [52] with solid-state PL maxima (λ_{em}) and photoluminescence quantum yields (Φ_{PL}).

The Schiff base derivatives **61**–**66** developed by the group of Zhou bear different terminal aromatic substituents on the BI moiety. All the compounds presented unusual AIE behavior. They were very weakly emissive in pure THF, but become strongly luminescent when adding between 30 and 60% v/v water in THF. Then, with increasing the water fraction, the PL intensity decreased again. Differences with sample aging were also observed. On the basis of electron microscopy observations, this effect was attributed to the formation of different types of aggregates, particularly sensitive to the environment, and to the growth of crystals that are much less emissive than aggregates [83].

Compound **67** differs from **52** (Fig. 15) by the presence of a TPA unit instead of the terminal carbazole unit. Both compounds have very close spectroscopic properties and sensitivity for acidic vapors. The gelation capacities are almost identical, which suggests that the second fatty chain on **52** does not play an important role in this property [78]. Compound **68** is also very close from the carbazole derivative **50** (Fig. 15) [52].

3.9 Boron derivatives and mechanofluorochromic effect

Benzazole derivatives may be used as ligands to form different types of boron complexes. The coordination with the boron center leads to a rigid and planar four- or three-ring-fused π-conjugated system, and enhances the donor-acceptor character of the molecule due to the intrinsic electron-withdrawing nature of the BF_2 group. These compounds may emit in the solid state, but like many closely-related boron-dipyrromethene (BODIPY) dyes, many of them are also strongly fluorescent in solution [84, 85]. For this reason, only one of the complexes reported by Meesala *et al*., i.e. compound **69**, may be consider showing AIE behavior with respect to THF/water mixtures (Fig. 18) [85].

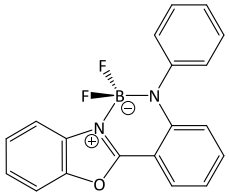

69 (agg) λ_{em} ~ 500 nm
(solid state) λ_{em} = 493 nm, Φ_{PL} = 0.20

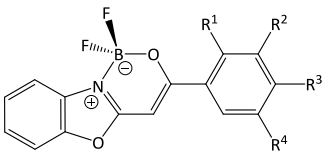

70 $R^1 = R^2 = R^3 = R^4$ = H (agg) λ_{em} = 468 nm; (powder) λ_{em} = 478 nm, Φ_{PL} = 0.49
71 $R^1 = OCH_3$, $R^2 = R^3 = R^4$ = H (agg) λ_{em} = 436/459 nm; (powder) λ_{em} = 439 nm, Φ_{PL} = 0.90
72 $R^1 = R^3 = R^4$ = H, $R^2 = OCH_3$ (agg) λ_{em} = 471 nm; (powder) λ_{em} = 462 nm, Φ_{PL} = 0.86
73 $R^1 = R^2 = R^4$ = H, $R^3 = OCH_3$ (agg) λ_{em} = 480/550 nm; (powder) λ_{em} = 480/550 nm, Φ_{PL} = 0.92
74 $R^1 = R^3 = OCH_3$, $R^2 = R^4$ = H (agg) λ_{em} = 476 nm; (powder) λ_{em} = 471 nm, Φ_{PL} = 0.80
75 $R^1 = R^4 = OCH_3$, $R^2 = R^3$ = H (agg) λ_{em} = 476 nm; (powder) λ_{em} = 466 nm, Φ_{PL} = 0.26
76 R^1 = H, $R^2 = R^3 = R^4 = OCH_3$ (agg) λ_{em} = 500 nm; (powder) λ_{em} = 505 nm, Φ_{PL} = 0.27

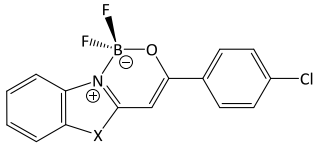

77 X = O (agg) λ_{em} = 492 nm, Φ_{PL} = 0.24
(pristine powder) λ_{em} = 447/472 nm
(after grinding) λ_{em} = 490 nm
78 X = S (solid state) λ_{em} = 522 nm
(pristine powder) λ_{em} = 461/490 nm
(after grinding) λ_{em} = 517 nm

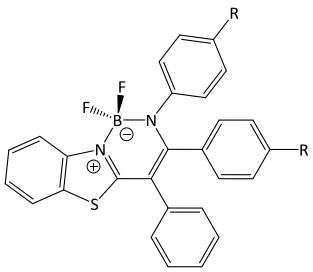

79 R = H (solid state) λ_{em} = 473 nm, Φ_{PL} = 0.60
80 R = $N(CH_3)_2$ (solid state) λ_{em} = 518 nm, Φ_{PL} = 0.27

Figure 18. Molecular structure of molecules **69** [85], **70**-**76** [86], **77** and **78** [87], **79** and **80** [88] with solid-state PL maxima (λ_{em}) and photoluminescence quantum yields (Φ_{PL}).

In contrast, this property is well expressed in the seven β-iminoenolate boron complexes **70**−**76** of Zhang *et al.*, the emission of which is quite weak in solution, but multiplied up to 91-fold for aggregates of **71**. Notably, for **73**, the color of the emitted light changed significantly with the nature of the aggregates formed. This compound also exhibited unusual multicolor emission upon grinding, reversible after solvent fuming [86].

The PBO-based complex **77** reported by Zhao *et al.* also exhibit distinct AIE behavior, while this is not the case for the PBT analogue **78**. However, both complexes are well emissive in the solid state and exhibit marked MFC. Their pristine crystals emit azure light, grinding turns their emitting colour into cyan and green, respectively, and the initial emitting colour is recovered under fuming or heating [87]. This type of MFC-active materials may find applications in anti-fake labels and mechanical strength sensors.

The geometry of the propeller-shaped BT-enamido boron difluoride complexes **79** and **80** is reminiscent to that of archetypical AIE-gens. The two solid compounds were strongly emissive, with PLQY of 0.60 and 0.27, much higher than in organic solvents (<0.01). The SLE effect is attributed to RIR of the three peripheral phenyl rings. Both complexes show MFC behavior, particularly marked for **80**, the maximum emission of which passes from 518 to 582 nm upon grinding, and conversely upon fuming with dichloromethane (Fig. 19). This compound is also very sensitive to hydrostatic pressure, the maximum emission of the pristine powder being gradually shifted till 645 nm at 10.34 GPa. This effect was attributed to co-planation of the propeller structure upon compression. Compound **80** has been proposed for use as a new piezochromic luminescence material [88].

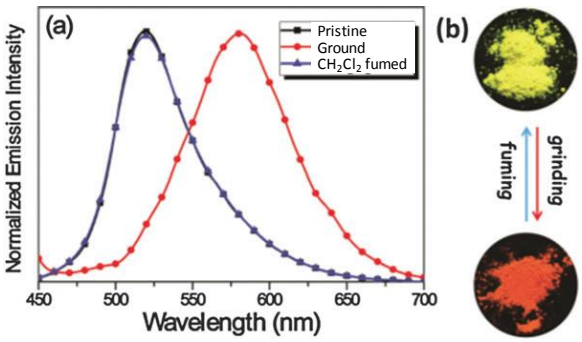

Figure 19. (a) Normalized luminescence spectra of solid compound **80**, after being ground and CH_2Cl_2 fumed, λ_{ex} 414 nm. (b) Photographs of the ground powder of **80** and the CH_2Cl_2-fumed ground powder under UV light (365 nm). Adapted from Ref. 88 with permission from the Royal Society of Chemistry.

4 Insertion of benzazole moieties in AIE-gen frameworks: Tuning and amplification of the AIE properties

4.1 Benzilideneimidazolinone derivatives

As seen above, BZ units may easily be converted into SLIE-fluorogens. However, another strategy is to merge these units with a well-known AIE-active unit. In molecules **81-86**, introduced by our team [89, 90], a PBO fragment has been combined with a synthetic derivative of the chromophore of the green fluorescent protein (GFP), i.e. *p*-hydroxybenzylideneimidazolinone (HBDI) (Fig. 20a). The HBDI chromophore is virtually not fluorescent in fluid medium, and emits blue-green light when constrained in a protein matrix, for example. However, the PLQY and photochemical stability of its derivatives are not always very good. The association with PBO strongly improves these properties. All compounds are weakly emissive in the blue region in fluid solvents. Time-dependent density functional theory (TD-DFT) and spin-flip TD-DFT calculations showed that the relaxation pathway in the lowest singlet excited state leads to a thermally-accessible conical intersection (CI), which favors

non-radiative deactivation. A strong twist of the imidazolinone moiety with respect to the rest of the molecule is necessary to access this CI. [91]. The long-chain PBO-BDI conjugates **82**–**86** displayed neat SLE enhancement with PLQY reaching 0.26 for the microcrystalline powders. The yellow-orange emission was shown to originate from long-distance excimers formed in the crystals [89]. Using a simple solvent-exchange method, these compounds easily form luminescent microfibers and non-doped nanoparticles [90]. The methyl derivative **81** was first assumed to be non-emissive in the solid state. However, crystallizing this molecule under precise experimental conditions allowed four distinct polymorphs and one solvate to be obtained. Three of these crystalline forms were indeed virtually not emissive, while the other two polymorphs exhibited strong photoluminescence (PL), close to that of the long-chain analogs. Recrystallization allowed for passing reversibly from one crystalline species to another. The non-emissive polymorphs are characterized by the presence of a centrosymmetric dimer structured by hydrogen bonds, in which paired molecules vibrate with the same mode and are in turn subjected to maximum deformation, according to DFT calculations. Vibrational dispersion of the excitation energy in the dimer, together with the easy access to CI permitted by a loose crystal structure, could explain the behavior of the three non-emissive polymorphs. In contrast, RACI may account for the PL emission of the other two species, which have tight crystal packing mode. The emergence of polymorphism and of a rare on/off PL mechanism may be attributed to the presence of the BDI unit in the molecule.

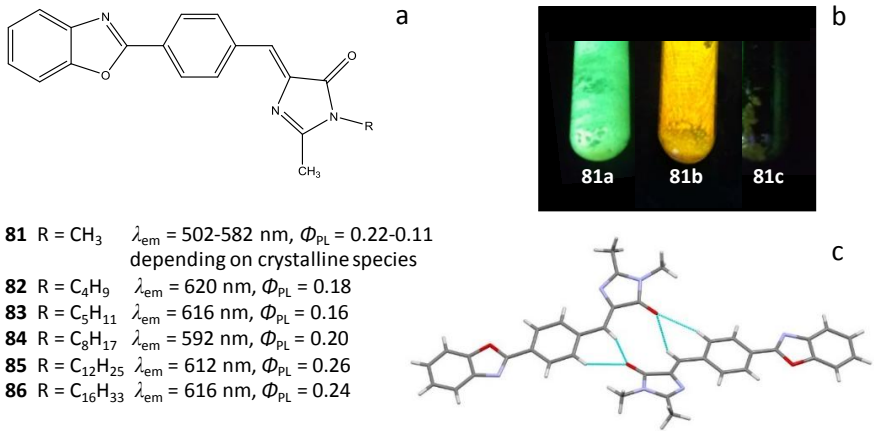

Figure 20. a) Molecular structure of molecules **81** [91], **82** and **83** [89], **84** [90], **85** [89] and **86** [90] with solid-state PL maxima (λ_{em}) and photoluminescence quantum yields (Φ_{PL}) of the microcrystalline powders. Image of the microcrystalline powders of two polymorph forms and one CH_3CN solvate (middle) of **81** excited at 365 nm. c) Example of dimer formed in the crystal structure of a non-emissive polymorph of **81**. Strong hydrogen bonds are drawn in blue ink.

4.2 Tetraphenylethene derivatives

Owing to its very simple structure, tetraphylethene or tetraphenylethylene (TPE) is the most popular representative of the anti-ACQ effect molecules. The modification of this building block has proven to be an efficient way to access new AIE-gens with valuable solid-state properties. The TPE molecule has been decorated with BZ units with the aim to tune its spectral properties. The design consists in the peripheral insertion of a BZ motif on one, two or even on each of the four phenyl groups of TPE. The BZ heterocycle is frequently attached to TPE by the carbon atom in the 2-position. More rarely, it is connected *via* a vinyl bond or a phenyl group. The BI can also be fixed to TPE by its nitrogen atom (Figs. 21 and 22).

From a general point of view, the TPE-BZ derivatives have a very good thermal stability, as illustrated by the molecules **87**–**90** and **91**–**94** developed by Zhang *et al.*, the decomposition temperature of which is above 319 and 340 °C, respectively [92, 93]. All TPE-BZ derivatives show weak emission in organic solution, and exhibit clear fluorescence enhancement in the aggregate state. In the solid state, TPE is a blue emitter (444-453 nm) [94, 95]. Molecules **87**–**90** and **91**–**94**, which

bear only one BI unit, also emit in the blue region at 440-454 nm [92] and ~461-467 nm [93], respectively. Molecule **95**, a highly conjugated π–system with four BI units, has a yellowish green

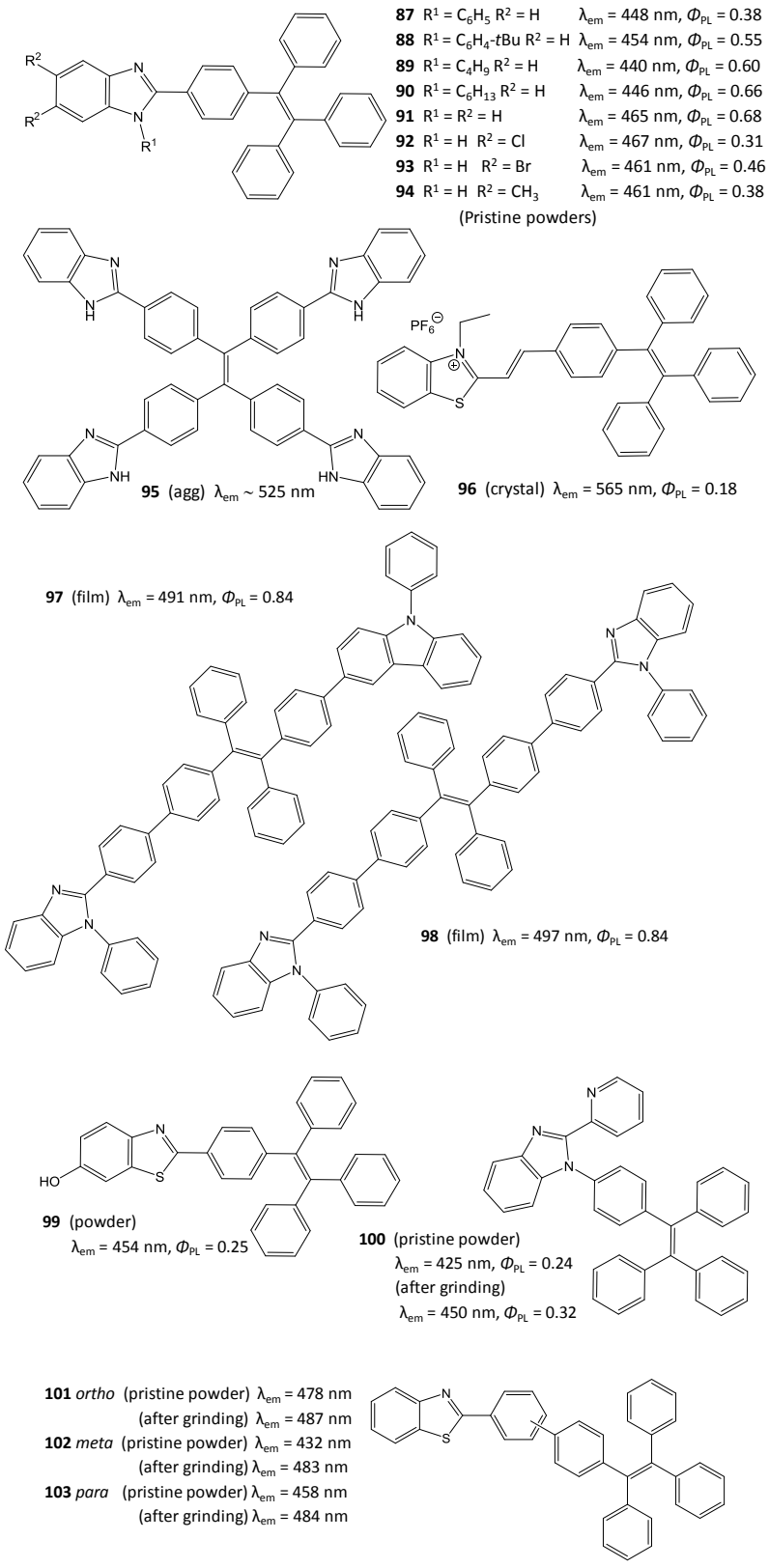

Figure 21. Molecular structure of TPE derivatives **87**–**90** [92], **91**–**94** [93], **95** [96], **96** [97], **97** and **98** [98], **99** [99], **100** [100] and **101**–**103** [101] with solid-state PL maxima (λ_{em}) and photoluminescence quantum yields (Φ_{PL}).

emission at 525 nm [96]. For the benzothiazolium derivative **96**, with strong ICT, the emission maximum is 565 nm for the pure dye, and 591 nm for a solvate [97]. However, the most stunning characteristic of some TPE-BZ derivatives is their very high PLQY, reaching for example 0.68 for **91** [93], 0.84 for **97** and 0.86 for **98** [98], while it is only 0.22 for TPE.

As may be expected, X-ray diffraction analyses of single crystals showed that all the TPE-BZ derivatives have highly twisted paddle-shaped conformations, considering the position of the four phenyl rings with respect to the central ethylene segment. In most of the molecules, the BI moiety and the adjacent phenyl ring of TPE are nearly planar, as is commonly the case in aryl-substituted BZ. This is not the case in sterically-hindered compounds **87**–**90**, where the torsion angle between the BI heterocycle and the phenyl ring is between 34 and 44° [92]. The crystal packing mode is different in every case. For example, molecules **91**, **92** and **94** form chain-like one-dimentional (1D) supramolecular structure [93], while **87**–**90** and **99** adopt a fashion stacking by 2-D layers [92, 99]. Slipped π-π intermolecular interactions may be observed [93], molecules are generally linked by affluent weak C-H-π and C-H-N intermolecular interactions. Above all, significant cavities and interface gaps are frequently mentioned, so that crystal packing interactions may be readily destroyed by mechanical stimuli. Indeed, the molecules cited above exhibit clear MFC effect. Upon grinding by a spatula or a pestle, the sky-blue emissive microcrystals of **87**–**90** and **91**–**94** convert to yellowish green emitting amorphous solids, and *vice versa* upon heating or fuming with dichloromethane vapors [92, 93]. The solid-state emission of crystals of **96** is reversibly tuned from yellow or orange to red by grinding and fuming or heating processes [97]. In the same conditions, molecule **100** reported by Cui *et al*. exhibits a color change from deep blue to turquoise [100]. Molecule **99** reported by Ma *et al*. exhibits remarkable four-colour switching, by combining grinding/solvent-fuming cycles with protonation/deprotonation cycles based on exposure to HCl and NH_3 vapor [99]. Finally, the three isomers **101**–**103** of Jadhav *et al*. allowed to show that the AIE and MFC properties depend on the linkage between BT and the TPE unit. The *meta* isomer shows the strongest bathochromic spectral shift (51 nm) upon grinding, while this effect was weaker for the *para* and *ortho* isomers (26 and 9 nm, respectively). It is noteworthy that molecules of the *ortho* isomer are more tightly twisted and packed in the crystals than those of the *meta* isomer [101]. For all these MFC-active compounds, applications in the fields of chemo- and mechanosensors, optical displays and rewritable optical media are envisaged.

The electroluminescence properties of **88** are attractive for use in OLEDs, for which the development of blue-emitting luminogens is still a challenge [92]. In this context, molecule **97** has been especially designed to combine three functional units, i.e. the AIE-gen building block TPE, the electron-transporting PBI and the hole-transporting carbazole. Indeed, **97** acts as a bipolar emitter that exhibits good SLE properties, and well-balanced electron-hole transport and recombination properties. Its non-doped OLEDs showed excellent performances, with maximum luminance, current efficiency, power efficiency and external maximum efficiency values that reach the theoretical limit for fluorescent OLEDs. This performance ise much better than that of the molecules that bear two identical PBI moieties (**98**), or two carbazole units on the central TPE unit [98].

Finally, applications in the field of sensors are also possible. The tetrasubstituted nitrogen-rich BI-TPE derivative **95** possesses high affinity for Ag(I) cations, with which it forms complexes having a 1:2 stoichiometry. In methanol solution, such complexes assemble in aggregates that emit strong yellow light. The method is quite selective with respect to other cations and it has been proposed for the facile determination of Ag(I) ions in environmental samples, with the aim of pollution control [96].

In molecules **104** (Fig. 22), merging TPE with HTZ allows the ESIPT process to be implemented. The SLE effect is dramatic. The molecule is weakly emissive in acetone, but its PLQY is 0.36 as aggregates in aqueous acetone, and 0.97 in the solid state. It exhibits a large Stokes shift, with emission from the keto form at 589 nm. Of course, this effect is not observed with the parent compound **105** and the methoxy derivative **106** that cannot show any ESIPT effect. A protection/deprotection strategy is implemented for the detection of biothiols such as cysteine, homocysteine and gluthathione that play critical roles in cells as antioxidants and signaling agents [102]. In compound **107**, the hydroxyl function is protected by a 2,4-dinitrobenzenesulfonyl group, which results in fluorescence quenching. Thiols induce the stoichiometric conversion of **107** into **104**,

whose aggregation in the medium turns on the PL response. The compound is usable on test strips with good specificity with respect to other analytes, and can even be used for the detection of biothiols in living cells [102]. Similarly, Liu *et al.* have developed the closely-related molecule **108**, in which the hydroxyl group is protected by a levulinate unit. This molecule has been successfully used to conduct the ratiometric imaging of endogeneous sulfur dioxide SO_2, a signal transduction agent involved in the regulation of the cardiovascular function, in mammalian cells, mouse embryonic fibroblasts, and zebrafish [103].

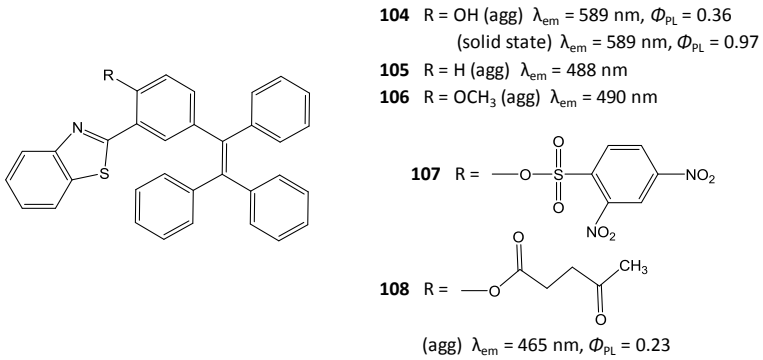

Figure 22. Molecular structure of TPE derivatives **104**–**106** [102] and **105**–**108** [103] with solid-state PL maxima (λ_{em}) and photoluminescence quantum yields (Φ_{PL}).

The AIE mechanism of TPE-based fluorophores has been well studied. Initially, the π-bond is destroyed upon excitation and a diradical species is generated. Then, two main processes may take place, depending on the molecular structure. The first one follows the RACI model, associated with double bond torsion. The second one involves the formation of a C-C bond between adjacent phenyl rings, leading to a photocyclized intermediate. The latter process requires large motion of the phenyl rings and is blocked in the aggregate phase [24–26].

5 A glance at synthesis

The demanding and complex synthesis of AIE molecular systems (commonly large rotor molecules with luminescence in the blue and green spectral region) is known to be a major drawback of this approach. In comparison, the synthesis of small BZ derivatives is much simpler. Through the examples given below, it can be seen that molecules exhibiting an effective SLE effect can be obtained in few steps with satisfactory yields.

The 2-arylbenzazole moieties are generally obtained by condensation of 2-aminophenol, 2-aminothiophenols or 1,2-diaminobenzene derivatives with carboxylic acids in the presence of polyphosphoric acid (PPA) or aldehydes. For example, Yadav *et al.* have been prepared the cyano derivatives **2**–**7** by classical Knovenaegel condensation of 4-(benzo[d]oxazol-2-yl)benzaldehyde with substituted isophorones, benzothiazole or benzimidazoles in the presence of piperidine (Scheme 1).

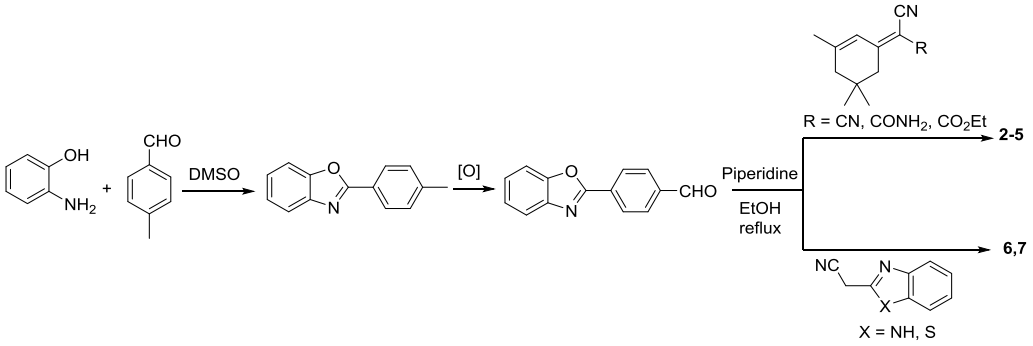

Scheme 1. Synthesis of cyano-derivatives **2**-**7** [44].

The 4'-formyl derivative of BPO was obtained following a two-step procedure with 2-(*p*-tolyl)benzo[d]oxazole intermediate formation and its subsequent low yield oxidation by toxic selenium dioxide or chromium trioxide [44].

Recently, our group has reported an improved procedure to access to formyl-BPO precursor by condensation of 2-aminophenol with terephtalaldehyde and subsequent treatment with 2,3-dichloro-5,6-dicyano-1,4-benzoquinone (DDQ) in 45% overall yield [45] (Scheme 2).

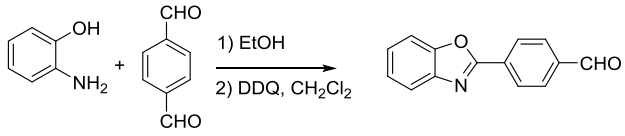

Scheme 2. Alternative synthesis of 4-(benzo[d]oxazol-2-yl)benzaldehyde [45].

The Schiff bases **10**-**12** were prepared in good yields (60 to 84%) from the condensation of *p*-(benzoxalzolyl)anilines (obtained from 2-aminophenol with *p*-aminobenzoic acid in PPA) with the required aromatic aldehydes in refluxing ethanol [54] (Scheme 3).

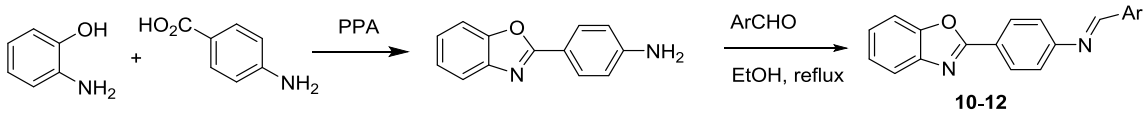

Scheme 3. Synthesis of Schiff bases **10**-**12** [54].

Similarly, the benzimidazole-based Schiff bases **14**–**16** were prepared from 2-aminobenzimidazole derivatives, readily obtained from the corresponding *o*-phenylenediamine and cyanogen bromide [56] (Scheme 4).

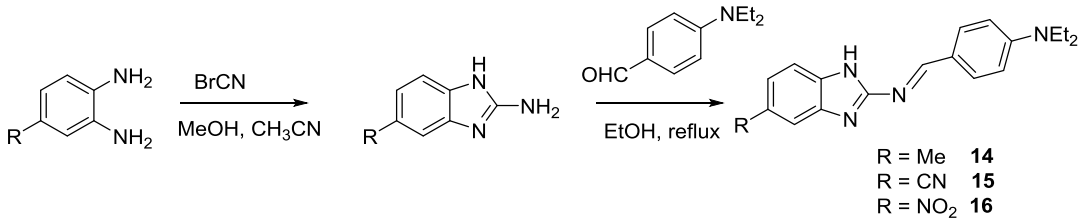

Scheme 4. Synthesis of Schiff bases **14**-**16** [56].

Organogelator **17**, which contains two benzimidazole moieties and an aromatic Schiff-base unit, was prepared by condensation in refluxing DMF of 1,4-phtalaldehyde with an acylhydrazide derivative obtained in two steps from 2-phenethylbenzimidazole [57]. Similarly, gelator **18**, based on an acylhydrazone naphtol moiety, resulted from the reaction of with 2-hydroxy naphthalene formaldehyde with the required benzimidazole acetylhydrazide derivative in refluxing ethanol [58] (Scheme 5).

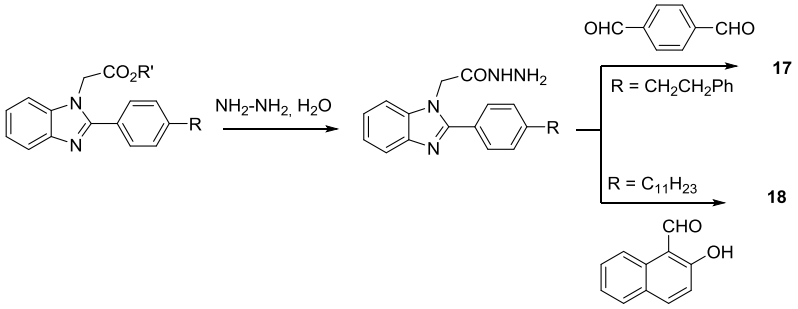

Scheme 5. Synthesis of organogelators **17** [57] and **18** [58].

Carboxamide benzoxazole derivatives **19** and **20** were classically obtained by coupling (benzoxalzolyl)anilines with 4-*tert*-butylbenzoic acid in the presence of *N*,*N*′-carbonyldiimidazole (CDI) in refluxing toluene [59, 60] (Scheme 6).

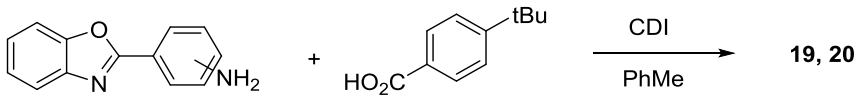

Scheme 6. Synthesis of carboxamide benzoxazole derivatives **19** [59] and **20** [60].

2'-Hydroxyphenyl-benzoxazole and benzothiazole derivatives come from the condensation of 2-aminophenol and 2-aminothiophenol, respectively, with an *o*-hydroxybenzoic acid reagent in the presence of PPA. Padalkar *et al.* developed an access to 2'-HBT derivatives by Pd-catalyzed Suzuki coupling reaction [74, 75]. The 2'-HBT framework was initially obtained from acid-catalyzed cyclization of 2-aminothiophenol and 4-bromo-2-hydroxybenzoic acid leading to intermediate 2-(benzo[*d*]thiazol-2-yl)-5-bromophenol in 52% yield. Coupling with various boronic acids in the presence of $Pd(Ph_3)_4$ and K_2CO_3 afforded a variety of carbazole, triphenylamine, fluorene derivatives.in moderate to good yields, as illustrated below for carbazole derivative **47** in scheme 7.

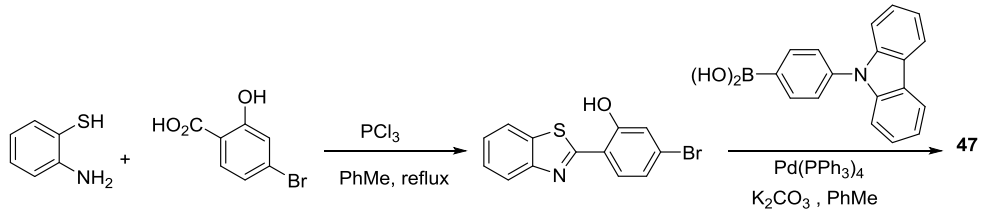

Scheme 7. Synthesis of 2'-hydroxyphenyl-benzothiazole derivative **47** [75].

A one-step Knoevenagel reaction was enough for Xue *et al.* to prepare the stilbene derivatives of carbazole-based (**51**) and phenothiazine benzoxazoles (**53**, **54**) in high 82 to 86% yield, starting from commercially available 2-methylbenzoxazole and carbazole or phenothiazine carbaldehydes in the presence of potassium *tert*-butoxide in THF [76, 79] (Scheme 8).

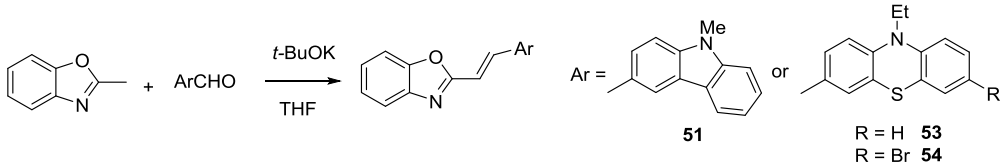

Scheme 8. Synthesis of stylbene benzoxazole derivatives **51** [76] and **53**–**54** [79].

The triphenylamine-containing benzimidazole derivatives **61**–**66** were prepared by Cao *et al.* by condensation of 4-[*bis*-(4-ethoxyphenyl)-amino]-benzaldehyde of with 4-nitro-benzene-1,2-diamine in refluxing DMF. Subsequent reduction of the nitro function and condensation with the requisite aldehydes provided the target Schiff bases [83] (Scheme 9).

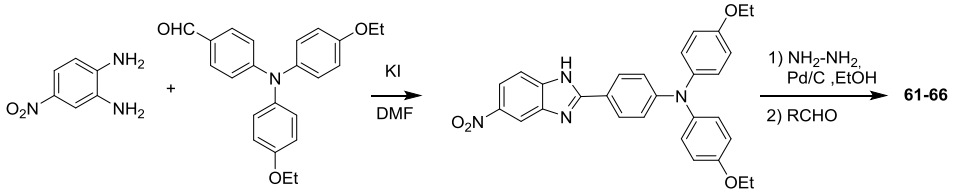

Scheme 9. Synthesis of triphenylamine-containing benzimidazole derivatives **61**–**66** [83].

In the same way, triphenylamine benzoxazole **55** was efficiently obtained by reaction of 2-methylbenzoxazole with 4-(diphenylamino)benzaldehyde in the presence of potassium *tert*-butoxide in THF with a yield of 86% [80] (Scheme 10).

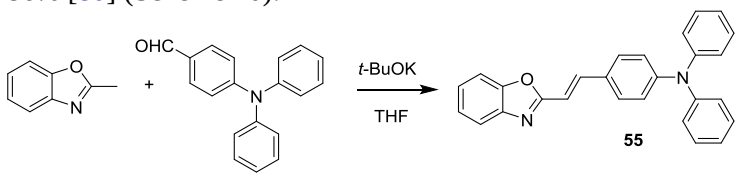

Scheme 10. Synthesis of triphenylamine benzoxazole **55** [80] **.**

The borate complexes were efficiently obtained by boron complexation at the chelating site of 2'-aminophenyl benzoxazole (for **69**) or *β*-ketoimidates derivatives after treatment with boron trifluoride diethyl etherate as exemplified for derivative **70**−**76** in the Scheme 11 [86].

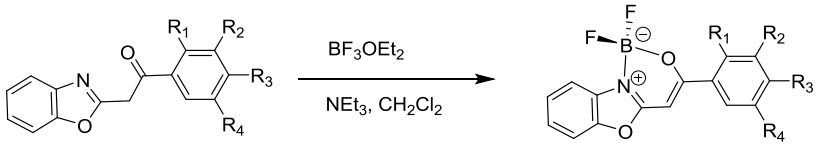

Scheme 11. Synthesis of boron complexes **70**−**76** [86].

Merging a BZ unit with a typical AIE-gen can also be achieved very simply. Ghodbane *et al.* efficiently synthetized a series of benzilideneimidazolinone derivatives **81**−**86** in a two-step procedure. Condensation of 2-(4′-formylphenyl)benzoxazole with a primary alkylamine led to the corresponding imino derivatives, and subsequent [2+3] cycloaddition reaction with methyl[(1-ethoxyethylidene)amino]acetate gave the target compounds in high yields [89−91] (Scheme 12).

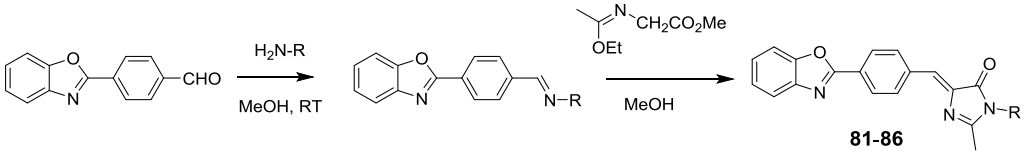

Scheme 12. Synthesis of benzilideneimidazolinone derivatives **81**−**86** [89−91].

Tetraphenylethene derivatives are generally obtained starting from functionalized bromo- or formyl- derivatives of TPE. For example, Zhang *et al.* synthetized compounds **91**−**94** in high yields starting from tetraphenylethene carbaldehydes by typical cyclisation with phenylenediamine derivatives [93] (Scheme 13).

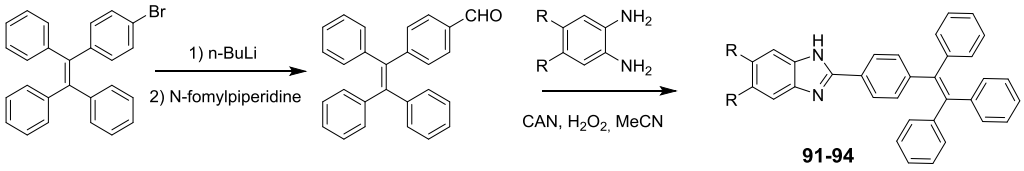

Scheme 13. Synthesis of TPE-BI derivatives **91**−**94** [93].

Likewise, TPE-based benzothiazoles such as **99** and **104**−**106** were prepared by reaction of 4-phenylethenealdehyde with the appropriate 2-aminobenzenethiols [99, 102]. The Suzuki Pd-catalyzed cross-coupling reaction was also well exploited to access TPE-BZ derivatives. For instance, compound **98** was obtained by Zhang *et al.* in 40% yield *via* a Suzuki coupling reaction between 1,2-bis(4-

bromophenyl)-1,2-diphenylethene and adequate commercially available phenylbenzimidazole boronic acid [98] (Scheme 14).

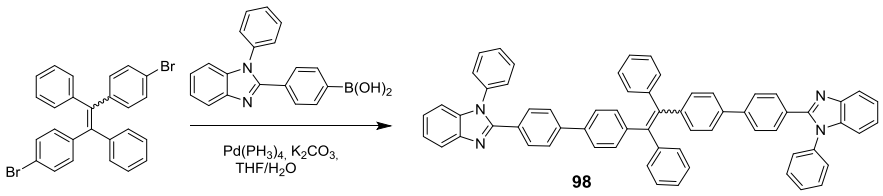

Scheme 14. Synthesis of derivative **98** [98].

Finally, it must be stressed that an access to tetra(hetero)arylethylene derivatives embedding benzoxazoles substituents has recently been developed by Tan *et al.* involving a *trans*-selective 1,2-diheteroarylation of diarylalkyne with benzoxazole *via* rhodium/copper co-catalyzed C-H addition/oxidative coupling process. The optimized conditions using [R Cp* $(MeCN)_3][SbF_6]_2$ as the catalyst, $Cu(OAc)_2$ as the oxidant, and pivalic acid as additive in dichloroethane efficiently yielded a large variety of compounds depending on the diaryl alkyne and azole derivatives used as starting materials [95] (Scheme 15). This synthetic procedure opens wide perspectives in the development of a new generation of SLE-active compounds.

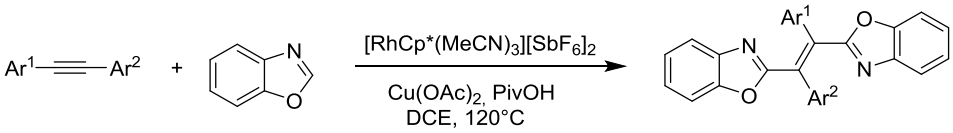

Scheme 15. Synthesis tetra(hetero)arylethylene derivatives. by addition/oxidative coupling of diaryl alkynes with benzoxazole [95].

6 Conclusion and perspectives

So far, BZ units do not belong to the small family of archetypical AIE-gens. However, they are at the basis of very efficient SLE-active molecules. Substituting a BZ heterocycle with a -C=C-Ar or -N=C-Ar moiety, or connecting a $C=CR^1R^2$, -C=NR or $-N=CR^1R^2$ group to an aryl-benzazole is sufficient to generate SLE properties. Benzazole moieties bring these properties to classical ACQ-active molecules, which in turn enhance the electroluminescence and MFC properties of the conjugate. Such molecules are attractive for use in OLEDs and as multi-responsive sensors. The ESIPT properties of the hydroxy derivatives allow the development of sensors based on a protection/deprotection strategy. Decoration of TPE with BZ motifs leads to molecules whose electroluminescent properties are close to the theoretical limit.

According to the size of the π-conjugated system, BZ derivatives cover a very broad range of wavelengths. They range from blue emitters, in high demand for OLEDs, to red emitters, very useful for biological imaging. Various types of solids may be obtained, from microcrystals to thin films. Many BZ derivatives also arrange spontaneously in nanofibers [7] and readily give organogels. The easy introduction of a variety of substituents allows the physicochemical properties to be finely tuned. It also allows controlling the crystal packing mode, given that the molecular arrangement is generally very favorable to the emission of light.

It may be surprising to see that BZ derivatives represent about half of the molecules reviewed above, while umpteen number of BT and BI derivatives have been reported for excellent fluorescent, thermal and mechanical properties that make them potential candidates for applications in the field of optically-active materials. This uneven distribution comes from the fact that BO has been used more frequently than the other two isologs in fundamental studies about SLE properties. However, BT and BI have been almost exclusively chosen when optoelectronic applications were researched. For other

applications, the three BZ could be more or less interchangeable, and the additional substitution possibility offered by BI may sometimes be an advantage.

Many developments are possible. SLE-active materials could be obtained by coupling BZ with other molecules, with the aim of generating new properties. It is known, for example, that crystals of some BZ-naphthalene derivatives exhibit photomechanical effect [104]. The conjugation with coumarins gives access to compounds with valuable non-linear optic (NLO) properties [105], while cyanines derivatives are NIR-emitting bio-probes [106]. There are many things to explore in the field of closely-related compounds, such as benzothiadiazole derivatives, which exhibit reversible mechanofluorochromism [107] and multi-stimuli responsiveness [108]. It is noteworthy that since benzothiadiazole cannot be substituted in the 2-position, the synthesis and architecture of the derivatives obtained are different from those of the BZ derivatives described above.

This article is focused on organic compounds. However, due to their very good metal-ion chelating properties, BZ units have also been used successfully as ligands in transition metal complexes that exhibit SLE behavior [109, 110]. Furthermore, BZ may be included into the organic ligand, without direct participation to the coordination sphere, and so they contribute to enhancing the SLE properties. This is the case for example for the SLE-active and mechanoresponsive rhenium(I) complexes developed in our group [111, 112]. A new avenue is opening up in the field of coordination chemistry. This topic surely deserves to be further developed.

At the moment, it is our hope that this review article has convinced the reader that benzazoles are precious building blocks for the design of very efficient luminescent materials based on small molecules, obtained from facile and economic synthesis.

Acknowledgements

This publication is part of a project that has received funding from Agence Nationale pour la Recherche (ANR), SUPERFON project # ANR-17-CE07-0029-03.

Conflict of interest statement

We declare no conflict of interest.

References

[1] Kamal U, Javed NM, Arun K (2020) Biological potential of benzoxazole derivatives: an updated review. Asian J Pharm Clin Res 13:28–41. DOI: 10.22159/ajpcr.2020.v13i8.37958

[2] Demmer CS, Bunch L (2015) Benzoxazoles and oxazolopyridines in medicinal chemistry studies. Eur J Med Chem 97:778–785. DOI: 10.1016/j.ejmech.2014.11.064

[3] Keri RS, Patil MR, Patil SA, Budagumpi S (2015) A comprehensive review in current developments of benzothiazole-based molecules in medicinal chemistry. Eur J Med Chem. 89:207–251. DOI: 10.1016/j.ejmech.2014.10.059

[4] Keri RS, Hiremathad A, Budagumpi S, Nagaraja BM (2015) Comprehensive Review in Current Developments of Benzimidazole-Based Medicinal Chemistry. Chem Biol Drug Des 86:799–845. DOI: 10.1111/cbdd.12462

[5] Krasovitskii BM, Bolotin BM (1988) Organic Luminescent Materials. Wiley-VCH Verlag GmbH, Weinheim. ISBN-13: 978-3527267286

[6] Chen SH, Jiang K, Xiao Y, Cao XY, Arulkumar M, Wang ZY (2020) Recent endeavors on design, synthesis, fluorescence mechanisms and applications of benzazole-based molecular probes toward miscellaneous species. Dyes Pigment 175: 108157. DOI: 10.1016/j.dyepig.2019.108157

[7] Carayon C, Fery-Forgues S. (2017) 2-Phenylbenzoxazole derivatives: a family of robust emitters of solid-state fluorescence. Photochem Photobiol Sci 16:1020–1035. DOI: 10.1039/c7pp00112f

[8] Mei J, Leung NLC, Kwok RTK, Lam JWY, Tang BZ (2015) Aggregation-Induced Emission: Together We Shine, United We Soar! Chem. Rev. 115:11718–11940. DOI: 10.1021/acs.chemrev.5b00263

[9] Zhao Z, Zhang H, Lam JWY, Tang BZ (2020) Aggregation-Induced Emission: New Vistas at the Aggregate Level. Angew Chem, Int Ed 59:9888–9907. DOI: 10.1002/anie.201916729

[10] Shi J, Aguilar Suarez LE, Yoon SJ, Varghese S, Serpa C, Park SY, Lüer, D. Roca-Sanjuán D, Milián-Medina B, Gierschner J (2017) Solid State Luminescence Enhancement in π-Conjugated Materials: Unraveling the Mechanism beyond the Framework of AIE/AIEE. J Phys Chem C 121:23166–23183. DOI: 10.1021/acs.jpcc.7b08060

[11] Anthony SP (2012) Organic solid-state fluorescence: Strategies for generating switchable and tunable fluorescent materials, ChemPlusChem 77:518−531. DOI: 10.1002/cplu.201200073

[12] Bera MK, Pal P, Malik S (2020) Solid-state emissive organic chromophores: design, strategy and building blocks. J Mater Chem C 8:788−802. DOI: 10.1039/c9tc04239c

[13] Dimitriev OP, Piryatinski YP, Yuri L. Slominskii YL (2018) Excimer Emission in J-Aggregates. J Phys Chem Lett 9:2138−2143. DOI: 10.1021/acs.jpclett.8b00481

[14] Wilbraham L, Louis M, Alberga D, Brosseau A, Guillot R, Ito F, Labat F, Métivier R, Allain C, Ciofini I (2018) Revealing the Origins of Mechanically Induced Fluorescence Changes in Organic Molecular Crystals. Adv Mater 30:1800817. DOI: 10.1002/adma.201800817

[15] Gierschner J, Shi J, Milián-Medina B, Roca-Sanjuán D, Varghese S, Park SY (2021) Luminescence in Crystalline Organic Materials: From Molecules to Molecular Solids. Adv Optical Mater 2002251. DOI: 10.1002/adom.202002251

[16] Gierschner J, Lüer L, Milián-Medina B, Oelkrug D, Egelhaaf HJ (2013) Highly Emissive H-Aggregates or Aggregation-Induced Emission Quenching? The Photophysics of All-Trans para-Distyrylbenzene. J Phys Chem Lett 4:2686−2697. DOI: 10.1021/jz400985t

[17] De Silva TPD, Sahasrabudhe G, Yang B, Wang CH, Chhotaray PK, Nesterov EE, Warner IM (2019) Influence of Anion Variations on Morphological, Spectral, and Physical Properties of the Propidium Luminophore. J Phys Chem A 123:111−119. DOI: 10.1021/acs.jpca.8b06948

[18] Andreiuk BA, Reisch A, Bernhardt E, Klymchenko AS (2019) Fighting Aggregation Caused Quenching and Leakage of Dyes in Fluorescent Polymer Nanoparticles: Universal Role of Counterion. Chem Asian J 14: 836−846. DOI: 10.1002/asia.201801592

[19] Soulié M, Carayon C, Saffon N, Blanc S, Fery-Forgues S (2016) A comparative study of nine berberine salts in the solid state: optimization of the photoluminescence and self-association properties through the choice of the anion. Phys Chem Chem Phys 18: 29999−30008. DOI: 10.1039/c6cp05848e

[20] Lu B, Fang X, Yan D (2020) Luminescent Polymorphic Co-crystals: A Promising Way to the Diversity of Molecular Assembly, Fluorescence Polarization, and Optical Waveguide. ACS Appl Mater Interfaces 12: 31940–31951. DOI: 10.1021/acsami.0c06794

[21] Bhowal R, Biswas S, Saseendran DPA, Koner AL, Chopra D (2019) Tuning the solid-state emission by co-crystallization through σ- and π-hole directed intermolecular interactions. CrystEngComm 21:1940–1947. DOI: 10.1039/c8ce02118j

[22] Jimbo T, Tsuji M, Taniguchi R, Sada K, Kokado K (2018) Control of Aggregation-Induced Emission from a Tetraphenylethene Derivative through the Components in the Co-crystal. Cryst Growth Des 18:3863−3869. DOI: 10.1021/acs.cgd.8b00141

[23] Kumar S, Singh M, Gaur P, Jou JH, Ghosh S (2017) Role of Voluminous Substituents in Controlling the Optical Properties of Disc/Planar-Like Small Organic Molecules: Toward Molecular Emission in Solid State. ACS Omega 2:5348−5356. DOI: 10.1021/acsomega.7b00832

[24] Crespo-Otero R, Li Q, Blancafort L (2019) Exploring Potential Energy Surfaces for Aggregation-Induced Emission-From Solution to Crystal. Chem Asian J 14:700–714. DOI: 10.1002/asia.201801649

[25] Chen Y, Lam JWY, Kwok RTK, Liu B, Tang BZ (2019) Aggregation-induced emission: fundamental understanding and future developments. Mater Horiz 6:428–433. DOI: 10.1039/c8mh01331d

[26] Rivera M, Stojanović L, Crespo-Otero R (2021) Role of Conical Intersections on the Efficiency of Fluorescent Organic Molecular Crystals. J Phys Chem A 125:1012−1024. DOI: 10.1021/acs.jpca.0c11072

[27] Presti D, Wilbraham L, Targa C, Labat F, Pedone A, Menziani MC, Ciofini I, Adamo C (2017) Understanding Aggregation-Induced Emission in Molecular Crystals: Insights from Theory. J Phys Chem C 121:5747–5752. DOI: 10.1021/acs.jpcc.7b00488

[28] Wang C, Li Z (2017) Molecular conformation and packing: their critical roles in the emission performance of mechanochromic fluorescence materials. Mater Chem Front 1:2174–2194. DOI: 10.1039/c7qM00201g

[29] Majumdar P, Tharammal F, Gierschner J, Varghese S (2020) Tuning Solid-State Luminescence in Conjugated Organic Materials: Control of Excitonic and Excimeric Contributions through π Stacking and Halogen Bond Driven Self-Assembly. ChemPhysChem 21:616–624. DOI: 10.1002/cphc.201901223

[30] Varughese S (2014) Non-covalent routes to tune the optical properties of molecular materials. J Mater Chem C 2:3499–3516. DOI: 10.1039/c3tc32414a

[31] Lu B, Liu S, Yan D (2019) Recent advances in photofunctional polymorphs of molecular materials. Chin Chem Lett 30:1908–1922. DOI: 10.1016/j.cclet.2019.09.012

[32] Tan R, Wang S, Lan H, Xiao S (2017) Polymorphism-Dependent and Mechanochromic Luminescent Molecules. Curr Org Chem 21:236–248. DOI: 10.2174/1385272820666160905104014

[33] Carayon C, André-Barrès C, Leygue N, Saffon-Merceron N, Boggio-Pasqua M, Fery-Forgues S (2021) The role of the synthetic chromophore of GFP in generating polymorphism-dependent on/off photoluminescence. Dyes Pigment 187, 109119. DOI: 10.1016/j.dyepig.2020.109119

[34] Sagara Y, Yamane S, Mitani M, Weder C, Kato T (2016) Adv Mater 28:1073–1095. DOI: 10.1002/adma.201502589

[35] Ma Z, Wang Z, Teng M, Xu Z, Jia X (2016) ChemPhysChem 16:1811–1828. DOI: 10.1002/cphc.201500181

[36] Khan F, Ekbote A, Misra R (2019) Reversible mechanochromism and aggregation induced enhanced emission in phenothiazine substituted tetraphenylethylene. New J Chem 43:16156–16163. DOI: 10.1039/c9nj03290h

[37] Khan F, Ekbote A, Mobin SM, Misra R (2021) Mechanochromism and Aggregation-Induced Emission in Phenanthroimidazole Derivatives: Role of Positional Change of Different Donors in a Multichromophoric Assembly. J Org Chem 86:1560−1574. DOI: 10.1021/acs.joc.0c02404

[38] Barman D, Gogoi R, Narang K, Iyer PK (2020) Recent Developments on Multi-Functional Metal-Free Mechanochromic Luminescence and Thermally Activated Delayed Fluorescence Organic Materials. Front Chem 8:483. DOI: 10.3389/fchem.2020.00483

[39] Su J, Fukaminato T, Placial JP, Onodera T, Suzuki R, Oikawa H, Brosseau A, Brisset F, Pansu R, Nakatani K, Métivier R (2016) Giant amplification of photoswitching by a few photons in fluorescent photochromic organic nanoparticles. Angew Chem Int Ed Engl 55: 3662−3666. DOI: 10.1002/anie.201510600

[40] Melnychuk N, Klymchenko AS (2018) DNA-Functionalized Dye-Loaded Polymeric Nanoparticles: Ultrabright FRET Platform for Amplified Detection of Nucleic Acids. J Am Chem Soc 140:10856–10865. DOI: 10.1021/jacs.8b05840

[41] Ghodbane A, D'Altério S, Saffon N, McClenaghan ND, Scarpantonio L, Jolinat P, Fery-Forgues S (2012) Facile access to highly fluorescent nanofibers and microcrystals via reprecipitation of 2-phenyl-benzoxazole derivatives. Langmuir 28:855–863. DOI: 10.1021/la2036554

[42] An BK, Gierschner J, Park SY (2012) π-Conjugated cyanostilbene derivatives: a unique self-assembly motif for molecular nanostructures with enhanced emission and transport. Acc Chem Res 45:544–54. DOI: 10.1021/ar2001952

[43] Carayon C, Ghodbane A, Leygue N, Wang J, Saffon-Merceron N, Brown R, Fery-Forgues S (2019) Mechanofluorochromic properties of an AIEE-active 2-phenylbenzoxazole derivative: More than meets the eye? ChemPhotoChem 3:545-553. DOI: 10.1002/cptc.201800261

[44] Yadav UN, Kumbhar HS, Deshpande SS, Sahoo SK, Shankarling GS (2015) Photophysical and thermal properties of novel solid state fluorescent benzoxazole based styryl dyes from a DFT study. RSC Adv 5:42971–42977. DOI: 10.1039/c4ra12908c

[45] Bremond E, Leygue N, Jaouhari T, Saffon-Merceron N, Erriguible A, Fery-Forgues S (2021) Effect of substitution on the solid-state fluorescence properties of styrylbenzoxazole derivatives with terminal dicyanomethylene group. J. Photochem. Photobiol. A 404:112857. DOI: 10.1016/j.jphotochem.2020.112857

[46] Suhina T, Amirjalayer S, Mennucci B, Woutersen S, Hilbers M, Bonn D, Brouwer AM (2016) Excited-state decay pathways of molecular rotors: twisted intermediate or conical intersection? J Phys Chem Lett 7:4285–4290. DOI: 10.1021/acs.jpclett.6b02277

[47] Willets KA, Callis PR, Moerner WE (2004) Experimental and theoretical investigations of environmentally sensitive single-molecule fluorophores. J Phys Chem B 108:10465–10473. DOI :10.1021/jp049684d

[48] Levine BG, Martínez TJ (2007) Isomerization through conical intersections. Annu Rev Phys Chem 58:613–634. DOI :10.1146/annurev.physchem.57.032905.104612

[49] Xue P, Yao B, Sun J, Zhang Z, Li K, Liu B, Lu R (2015) Crystallization-induced emission of styrylbenzoxazole derivate with response to proton. Dyes Pigment 112:255e261. DOI: 10.1016/j.dyepig.2014.07.026

[50] Horak E, Vianello R, Hranjec M, Krištafor S, Karminski Zamola G, Steinberg IM (2017) Benzimidazole acrylonitriles as multifunctional push-pull Chromophores: Spectral characterisation, protonation equilibria and nanoaggregation in aqueous solutions. Spectrochim Acta A 178:225–233. DOI: 10.1016/j.saa.2017.02.011

[51] Horak E, Hranjec M, Vianello R, Steinberg IM (2017) Reversible pH switchable aggregation-induced emission of self-assembled benzimidazole-based acrylonitrile dye in aqueous solution. Dyes Pigment 142:108−115. DOI: 10.1016/j.dyepig.2017.03.021

[52] Jana P, Yadav M, Kumar T, Kanvah S (2021) Benzimidazole-acrylonitriles as chemosensors for picric acid detection. J Photochem Photobiol A 404:112874. DOI: 10.1016/j.jphotochem.2020.112874

[53] Mishra A, Thangamani A, Chatterjee S, Chipem FAS, Krishnamoorthy G (2013) Photoisomerization of trans-2-[4′-(Dimethylamino)styryl]benzothiazole. Photochem Photobiol 89:247–252. DOI: 10.1111/j.1751-1097.2012.01227.x

[54] Wang L, Zheng Z, Yu Z, Zheng J, Fang M, Wu J, Tian Y, Zhou H (2013) Schiff base particles with aggregation-induced enhanced emission: random aggregation preventing π–π stacking. J Mater Chem C 1:6952–6959. DOI: 10.1039/c3tc31626b

[55] Wang L, Shen Y, Yang M, Zhang X, Xu W, Zhu Q, Wu J, Tian Y, Zhou H (2014) Novel highly emissive H-aggregates with aggregate fluorescence change in a phenylbenzoxazole-based system. Chem Commun 50:8723-8726. DOI: 10.1039/c4cc02564d

[56] Horak E, Robić M, Šimanović A, Mandić V, Vianello R, Hranjec M, Steinberg IM (2019) Tuneable solid-state emitters based on benzimidazole derivatives: Aggregation induced red emission and mechanochromism of D-π-A fluorophores. Dyes Pigment 162:688–696. DOI: 10.1016/j.dyepig.2018.10.069

[57] Ma X, Xie J, Tanga N, Wu J (2016) AIE-caused luminescence of a thermally-responsive supramolecular organogel. New J Chem 40:6584–658710. DOI: 10.1039/c6nj01211f

[58] Yao H, Wang J, Song SS, Fan YQ, Guan XW, Zhou Q, Wei TB, Lin Q, Zhang YM (2018) A novel supramolecular AIE gel acts as a multi-analyte sensor array. New J Chem 42:18059–18065. DOI: 10.1039/c8nj04160a

[59] Li J, Qian Y, Xie L, Yi Y, Li W, Huang W (2015) From dark TICT state to emissive *quasi*-TICT state: The AIE mechanism of *N*-(3-(benzo[*d*]oxazol-2-yl)phenyl)-4-*tert*-butylbenzamide. J Phys Chem C 119:2133−2141. DOI: 10.1021/jp5089433

[60] Qian Y, Cai M, Zhou X, Gao Z, Wang X, Zhao Y, Yan X, Wei W, Xie L, Huang W (2012) More than restriction of twisted intramolecular charge transfer: Three-dimensional expanded #-shaped cross-molecular packing for emission enhancement in aggregates. J Phys Chem C 116:12187−12195. DOI: 10.1021/jp212257f

[61] Zhao J, Ji S, Chen Y, Guo H, Yang P (2012) Excited state intramolecular proton transfer (ESIPT): from principal photophysics to the development of new chromophores and applications in fluorescent molecular probes and luminescent materials. Phys Chem Chem Phys14:8803–8817. DOI: 10.1039/c2cp23144a

[62] Padalkar VS, Seki S (2016) Excited-state intramolecular proton-transfer (ESIPT)-inspired solid state emitters. Chem Soc Rev 45:169–202. DOI: 10.1039/C5CS00543D

[63] Sedgwick AC, Wu L, Han HH, Bull SD, He XP, James TD, Sessler JL, Tang BZ, Tian H, Yoon J (2018) Excited-state intramolecular proton-transfer (ESIPT) based fluorescence sensors and imaging agents. Chem Soc Rev 47:8842—8880. DOI: 10.1039/c8cs00185e

[64] Syetov Y (2013) Luminescence spectrum of 2-(2'-hydroxyphenyl)benzoxazole in the solid state, Ukr J Phys Opt 14:1-5. DOI: 10.3116/16091833/14/1/1/2013

[65] Li G, Zhu D, Liu Q, Xue L, Jiang H (2013) Rapid detection of hydrogen peroxide based on aggregation induced ratiometric fluorescence change. Org Lett 15:924–927. DOI: 10.1021/ol4000845

[66] Hu R, Li S, Zeng Y, Chen J, Wang S, Li Y, Yang G (2011) Understanding the aggregation induced emission enhancement for a compound with excited state intramolecular proton transfer character. Phys Chem Chem Phys 13:2044–2051. DOI: 10.1039/c0cp01181a

[67] Gao M, Wang L, Chen J, Li S, Lu G, Wang L, Wang Y, Ren L, Qin A, Tang BZ (2016) Aggregation-Induced Emission Active Probe for Light-Up Detection of Anionic Surfactants and Wash-Free Bacterial Imaging. Chem Eur J 22:5107–5112. DOI: 10.1002/chem.201505202

[68] Feng X, Tong B, Shi J, Zhao C, Cai Z, Dong Y (2021) Recent progress of aggregation-induced emission luminogens (AIEgens) for bacterial detection and theranostics. Mater Chem Front 5:1164–1184. DOI: 10.1039/d0qm00753f

[69] Kim TH, Choi MS, Sohn BH, Park SY, Lyood WS, Lee TS (2008) Gelation-induced fluorescence enhancement of benzoxazole-based organogel and its naked-eye fluoride detection. Chem Commun 2364–2366. DOI : 10.1039/b800813b

[70] Chen H, Feng Y, Deng GJ, Liu ZX, He YM, Fan QH (2015) Fluorescent dendritic organogels based on 2-(2'-hydroxyphenyl)benzoxazole: Emission enhancement and multiple stimuli-responsive properties. Chem Eur J 21:11018–11028. DOI: 10.1002/chem.201500849

[71] Qian Y, Li S, Wang Q, Sheng X, Wu S, Wang S, Lia J, Yang G (2012) A nonpolymeric highly emissive ESIPT organogelator with neither dendritic structures nor long alkyl/alkoxy chains. Soft Matter 8:757–764. DOI: 10.1039/c1sm06358h

[72] Benelhadj K, Muzuzu W, Massue J, Retailleau P, Charaf-Eddin A, Laurent AD, Jacquemin D, Ulrich G, Ziessel R (2014) White emitters by tuning the excited-state intramolecular proton-transfer fluorescence emission in 2-(2'-hydroxybenzofuran)benzoxazole dyes. Chem Eur J 20:12843–12857. DOI: 10.1002/chem.201402717

[73] Kachwal V, Krishna ISV, Fageria L, Chaudhary J, Roy RK, Chowdhury R, Laskar IR (2018) Exploring the hidden potential of a benzothiazolebased Schiff-base exhibiting AIE and ESIPT and its activity in pH sensing, intracellular imaging and ultrasensitive & selective detection of aluminium (Al3+). Analyst 143:3741–3748. DOI: 10.1039/c8an00349a

[74] Padalkar VS, Sakamaki D, Tohnai N, Akutagawa T, Sakai K, Seki S (2015) Highly emissive excited-state intramolecular proton transfer (ESIPT) inspired 2-(2'-hydroxy)benzothiazole-fluorene motifs: spectroscopic and photophysical properties investigation. RSC Adv. 5:80283–80296. DOI: 10.1039/c5ra17980g

[75] Padalkar VS, Kuwada K, Sakamaki D, Tohnai N, Akutagawa T, Sakai K, Sakurai T, Seki S (2017) AIE Active Carbazole-Benzothiazole Based ESIPT Motifs: Positional Isomers Directing the Optical and Electronic Properties ChemSelect 2:1959–1966. DOI: 10.1002/slct.201602044

[76] Xue P, Yao B, Wang P, Sun J, Zhang Z, Lu R (2014) Response of strongly fluorescent carbazole-based benzoxazole derivatives to external force and acidic vapors. RSC Adv 4: 58732–58739. DOI: 10.1039/c4ra10330k

[77] Xue P, Yao B, Sun J, Zhang Z, Lu R (2014) Emission enhancement of a coplanar π-conjugated gelator without any auxiliary substituents. Chem Commun 50:10284–10286. DOI : 10.1039/c4cc04869e

[78] Wu Z, Sun J, Zhang Z, Gong P, Xue P, Lu R (2016) Organogelation of cyanovinylcarbazole with terminal benzimidazole: AIE and response for gaseous acid. RSC Adv 6:97293–97301. DOI: 10.1039/c6ra20910f

[79] Xue P, Yao B, Sun J, Xu Q, Chen P, Zhang Z, Lu R (2014) Phenothiazine-based benzoxazole derivates exhibiting mechanochromic luminescence: the effect of a bromine atom. J Mater Chem C **2**:3942–3950. DOI: 10.1039/c4tc00061g

[80] Xue P, Chen P, Jia J, Xu Q, Sun J, Yao B, Zhang Z, Lu R (2014) A triphenylamine-based benzoxazole derivative as a high-contrast piezofluorochromic material induced by protonation. Chem Commun 50:2569–2571. DOI: 10.1039/c3cc49208g

[81] Padalkar VS, Sakamaki D, Kuwada K, Tohnai N, Akutagawa T, Sakai K, Seki S (2016) AIE active triphenylamine–benzothiazole based motifs: ESIPT or ICT emission. RSC Adv 6: 26941–26949. DOI: 10.1039/c6ra02417c

[82] Padalkar VS, Sakamaki D, Kuwada K, Horio A, Okamoto H, Tohnai N, Akutagawa T, Sakai K, Seki S (2016) π–π Interactions: Influence on Molecular Packing and Solid-State Emission of ESIPT and non-ESIPT Motifs. Asian J Org Chem 5:938–945. DOI: 10.1002/ajoc.201600159

[83] Cao Y, Yang M, Wang Y, Zhou HP, Zheng J, Zhang X, Wu J, Tian Y, Wu Z (2014) Aggregation-induced and crystallization-enhanced emissions with time-dependence of a new Schiff-base family based on benzimidazole. J Mater Chem C 2:3686–3694. DOI: 10.1039/c3tc32551b

[84] Massue J, Frath D, Retailleau P, Ulrich G, Ziessel R (2013) Synthesis of Luminescent Ethynyl-Extended Regioisomers of Borate Complexes Based on 2-(2'-Hydroxyphenyl)benzoxazole. Chem Eur J 19:5375–5386. DOI: 10.1002/chem.201203625

[85] Meesala Y, Kavala V, Chang HC, Kuo TS, Yao CF, Lee WZ (2015) Synthesis, structures and electrochemical and photophysical properties of anilido-benzoxazole boron difluoride (ABB) complexes. Dalton Trans 44:1120–1129. DOI: 10.1039/c4dt03052d

[86] Zhang Z, Wu Z, Sun J, Xue P, Lu R (2016) Multi-color solid-state emission of β-iminoenolate boron complexes tuned by methoxyl groups : aggregation-induced emission and mechanofluorochromism. RSC Adv 6, 43755–43766. DOI: 10.1039/c6ra03722d

[87] Zhao J, Peng J, Chen P, Wang H, Xue P, Lu R (2018) Mechanofluorochromism of difluoroboron β-ketoiminate boron complexes functionalized with benzoxazole and benzothiazole. Dyes Pigment 149, 276–283. DOI: 10.1016/j.dyepig.2017.10.007

[88] Wang X, Liu Q, Yan H, Liu Z, Yao M, Zhang Q, Gong S, He W (2015) Piezochromic luminescence behaviors of two new benzothiazole–enamido boron difluoride complexes: intra- and inter-molecular effects induced by hydrostatic compression. Chem Commun 51, 7497–7500. DOI: 10.1039/c5cc01902h

[89] Ghodbane A, Fellows WB, Bright J, Ghosh D, Saffon N, Tolbert LM, Fery-Forgues S, Solntsev KM (2016) Effects of the benzoxazole group on green fluorescent protein chromophore crystal structure and solid state photophysics. J Mater Chem C 14:2793–2801. DOI: 10.1039/c5tc03776j

[90] Carayon C, Ghodbane A, Gibot L, Dumur R, Wang J, Saffon N, Rols MP, Solntsev KM, Fery-Forgues S (2016) Conjugates of benzoxazole and GFP chromophore with aggregation-induced enhanced emission: Influence of the chain length on the formation of particles and on the dye uptake by living cells. Small 12:6602–6612. DOI: 10.1002/smll.201602799

[91] Carayon C, André-Barrès C, Leygue N, Saffon-Merceron N, Boggio-Pasqua M, Fery-Forgues S (2021) The role of the synthetic chromophore of GFP in generating polymorphism-dependent on/off photoluminescence. Dyes Pigment, on press. DOI: 10.1016/j.dyepig.2020.109119

[92] Zhang T, Zhang R, Zhao Y, Ni Z (2018) A new series of N-substituted tetraphenylethene-based benzimidazoles: Aggregation-induced emission, fast-reversible mechanochromism and blue electroluminescence. Dyes Pigment 148:276e285. DOI: 10.1016/j.dyepig.2017.09.018

[93] Zhang T, Zhang R, Zhang Z, Ni Z (2016) A series of tetraphenylethene-based benzimidazoles: syntheses, structures, aggregation-induced emission and reversible mechanochromism. RSC Adv 6, 79871–79878. DOI: 10.1039/c6ra16514a

[94] Shi,J, Chang,N, Li C, Mei J, Deng C, Luo X, Liu Z, Bo Z, Dong YQ, Tang BZ (2012) Locking the phenyl rings of tetraphenylethene step by step: understanding the mechanism of aggregation-induced emission. Chem Commun 48:10675-10677. DOI: 10.1039/C2CC35641D

[95] Tan G, Zhu L, Liao X, Lan Y, You J (2017) Rhodium/Copper Cocatalyzed Highly trans-Selective 1,2-Diheteroarylation of Alkynes with Azoles via C−H Addition/Oxidative Cross-Coupling: A Combined Experimental and Theoretical Study. J Am Chem Soc 139: 15724–15737. DOI: 10.1021/jacs.7b07242

[96] Lu Z, Liu Y, Lu S, Li Y, Liu X, Qin Y, Zheng L (2018) A highly selective TPE-based AIE fluorescent probe is developed for the detection of Ag^{+}. RSC Adv 8:19701–19706. DOI: 10.1039/c8ra03591a

[97] Zhao N, Yang Z, Lam JWY, Sung HHY, Xie N, Chen S, Su H, Gao M, Williams ID, Wong KS, Tang BZ (2012) Benzothiazolium-functionalized tetraphenylethene: an AIE luminogen with tunable solid-state emission. Chem Commun 48:8637–8639. DOI: 10.1039/c2cc33780k

[98] Zhang J, Bai Y, Wei Q, Cao L, Wang T, Ge Z (2020) Efficient bipolar AIE emitters for high-performance nondoped OLEDs. J Mater Chem C 8, 11771–11777. DOI: 10.1039/d0tc02566f

[99] Ma C, Xu B, Xie G, He J, Zhou X, Peng B, Jiang L, Xu B, Tian W, Chi Z, Liu S, Zhang Y, Xu J (2014) An AIE-active luminophore with tunable and remarkable fluorescence switching based on the piezo and protonation–deprotonation control. Chem Commun 50:7374–7377. DOI: 10.1039/c4cc01012d

[100] Cui Y, Yin YM, Cao HT, Zhang M, Shan GG, Sun HZ, Wu Y, Su ZM, Xie WF (2015) Efficient piezochromic luminescence from tetraphenylethene functionalized pyridine-azole derivatives exhibiting aggregation-induced emission. Dyes Pigment 119:62e69. DOI: 10.1016/j.dyepig.2015.03.024

[101] Jadhav T, Dhokale B, Mobin SM, Misra R (2015) Mechanochromism and aggregation induced emission in benzothiazole substituted tetraphenylethylenes: a structure function correlation. RSC Adv 5:29878–29884. DOI: 10.1039/c5ra04881h

[102] Chen Q, Jia C, Zhang Y, Du W, Wang Y, Huang Y, Yang Q, Zhang Q (2017) A novel fluorophore based on the coupling of AIE and ESIPT mechanisms and its application in biothiol imaging. J Mater Chem B 5:7736−7742. DOI: 10.1039/c7tb02076g

[103] Liu Y, Nie J, Niu J, Wang W, Lin W (2018) An AIE + ESIPT ratiometric fluorescent probe for monitoring sulfur dioxide with distinct ratiometric fluorescence signals in mammalian cells, mouse embryonic fibroblast and zebrafish. J Mater Chem B 6:1973–1983. DOI: 10.1039/c8tb00075a

[104] Peng J, Ye K, Liu C, Sun J, Lu R (2019) The photomechanic effects of the molecular crystals based on 5-chloro-2-(naphthalenylvinyl)benzoxazols fueled by topo-photochemical reactions. J Mater Chem C 7:5433–544. DOI: 10.1039/c9tc01084j

[105] Sun J, Zheng M, Jia J, Wang W, Cui Y, Gao J (2019) New Coumarin-benzoxazole derivatives: Synthesis, photophysical and NLO properties. Dyes Pigment 164:287–295. DOI : j.dyepig.2019.01.010

[106] Dahal D, McDonald L, Bi XM, Abeywickrama C, Gombedza F, Konopka M, Paruchuri S, Pang Y (2017) An NIR-emitting lysosome-targeting probe with large Stokes shift via coupling cyanine and excited-state intramolecular proton transfer. Chem Commun 53:3697–3700. DOI: 10.1039/c7cc00700k

[107] Gautam P, Maragani R, Mobina SM, Misra R (2014) Reversible mechanochromism in dipyridylamine-substituted unsymmetrical benzothiadiazoles. RSC Adv 4, 52526−52529. DOI: 10.1039/C4RA09921D

[108] Jadhav T, Dhokale B, Patil Y, Mobin SM, Misra R (2016) Multi-Stimuli Responsive Donor−Acceptor Tetraphenylethylene Substituted Benzothiadiazoles. J Phys Chem C 120:24030−24040. DOI: 10.1021/acs.jpcc.6b09015

[109] Mao S, Han X, Li C, Huang G, Shen K, Shi X, Wu H (2018) Synthesis, crystal structure, fluorescence and electrochemical properties of two Ag(I) complexes based on 2-(4'-pyridyl)-benzoxazole/$SPPh_3$ ligands. J Coord Chem 71:3330–3341. DOI: 10.1080/00958972.2018.1514116

[110] Chai W, Hong M, Song L, Jia G, Shi H, Guo J, Shu K, Guo B, Zhang Y, You W, Chen X (2015) Three Reversible Polymorphic Copper(I) Complexes Triggered by Ligand Conformation: Insights into Polymorphic Crystal Habit and Luminescent Properties. Inorg Chem 54:4200−4207. DOI: 10.1021/ic502709b

[111] Wang J, Poirot A, Delavaux-Nicot B, Wolff M, Mallet-Ladeira S, Calupitan JP, Allain C, Benoist E, Fery-Forgues S (2019) Optimization of aggregation-induced phosphorescence enhancement in mononuclear tricarbonyl Rhenium(I) complexes: The influence of steric hindrance and isomerism. Dalton Trans 48:15906–15916. DOI: 10.1039/c9dt02786f

[112] Calupitan JP, Poirot A, Wang J, Delavaux-Nicot B, Wolff M, Jaworska M, Métivier R, Benoist E, Allain C, Fery-Forgues S (2021) Mechanical modulation of the solid-state luminescence of tricarbonyl rhenium(I) complexes through the interplay between two triplet excited states. Chem Eur J 27:4191– 4196. DOI: 10.1002/chem.202005245